

Synthesis and reactivity of iridium complexes of a macrocyclic PNP pincer ligand

Thomas M. Hood and Adrian B. Chaplin*

Department of Chemistry, University of Warwick, Gibbet Hill Road, Coventry CV4 7AL, UK

Email: a.b.chaplin@warwick.ac.uk

Table of Contents

1	Preparation of $[\text{Ir}(\text{PNP-14})(\eta^2:\eta^2\text{-COD})][\text{BAR}^{\text{F}}_4]$ (1)	2
2	NMR scale reaction of 1 with dihydrogen	3
3	Preparation of $[\text{Ir}(\text{PNP-14})(\text{biph})][\text{BAR}^{\text{F}}_4]$ (2)	4
4	NMR scale reactions of 2	6
4.1	Synthesis of $[\text{Ir}(\text{PNP-14})(2\text{-biphenyl})\text{H}][\text{BAR}^{\text{F}}_4]$ (3)	6
4.2	Synthesis of $[\text{Ir}(\text{PNP-14})\text{H}_2(\text{H}_2)][\text{BAR}^{\text{F}}_4]$ (4)	7
4.3	Synthesis of $[\text{Ir}(\text{PNP-14})\text{H}_2(\text{C}_2\text{H}_4)][\text{BAR}^{\text{F}}_4]$ (5)	8
4.4	Synthesis of $[\text{Ir}(\text{PNP-14})(\text{C}_2\text{H}_4)_2][\text{BAR}^{\text{F}}_4]$ (6)	9
4.5	Synthesis and isolation of $[\text{Ir}(\text{PNP-14})(\text{CO})][\text{BAR}^{\text{F}}_4]$ (8)	10
5	NMR scale reaction of $[\text{Ir}(\text{PNP-}t\text{Bu})(\text{biph})][\text{BAR}^{\text{F}}_4]$ (II) with dihydrogen	12
6	Preparation of $[\text{Ir}(\text{PNP-14}^*)\text{H}][\text{BAR}^{\text{F}}_4]$ (7)	13
7	NMR scale reaction of 7 with dihydrogen	15
8	Catalytic homocoupling of 3,3-dimethylbutyne promoted by 1	16
9	Catalytic homocoupling of 3,3-dimethylbutyne promoted by 6	19
10	Preparation of $[\text{Ir}(\text{PNP-14})(\eta^3\text{-}E\text{-C}(\text{C}\equiv\text{C}t\text{Bu})\text{CH}t\text{Bu})(\eta^1\text{-}E\text{-CHCH}t\text{Bu})][\text{BAR}^{\text{F}}_4]$ (10)	21
11	NMR scale reaction of 1 with $Z\text{-}t\text{BuC}\equiv\text{CCHCH}t\text{Bu}$	24
12	Synthesis and characterisation of $[\text{Rh}(\text{PNP-14})(\eta^2\text{-norbornene})][\text{BAR}^{\text{F}}_4]$	24

1 Preparation of $[\text{Ir}(\text{PNP-14})(\eta^2\text{-}\eta^2\text{-COD})][\text{BAR}^{\text{F}}_4]$ (1)

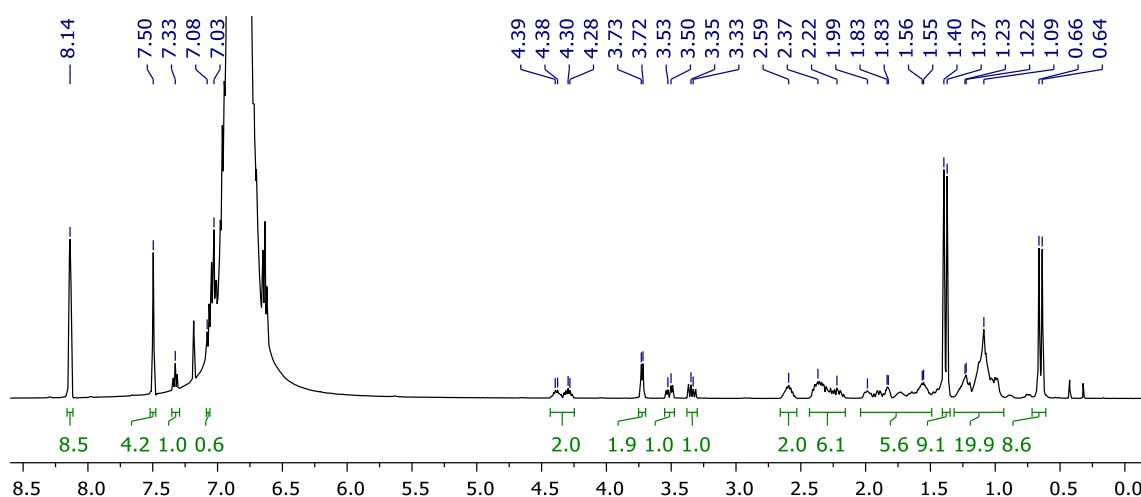


Figure S1. ^1H NMR spectrum of **1** (DFB, 500 MHz).

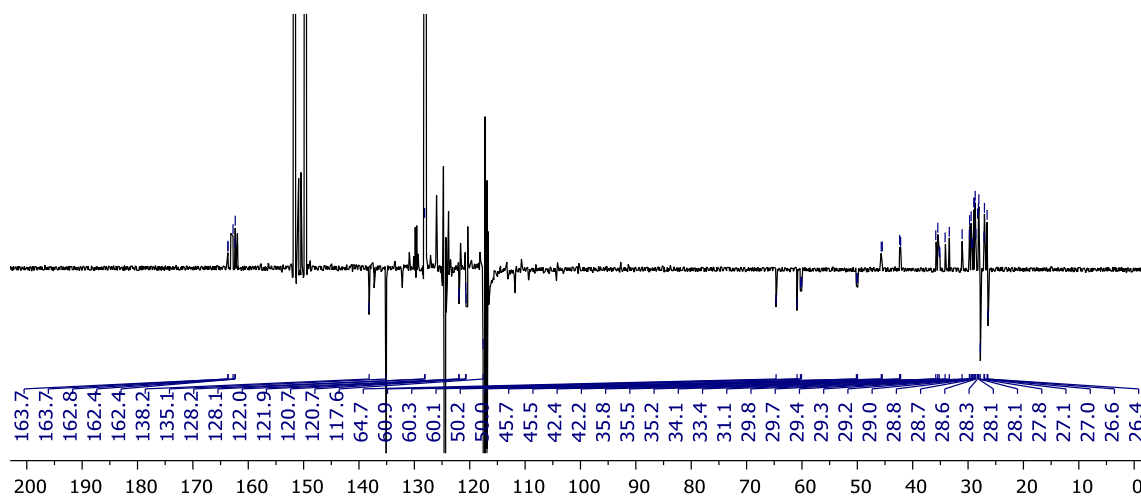


Figure S2. $^{13}\text{C}\{^1\text{H}\}$ APT NMR spectrum of **1** (DFB, 126 MHz).

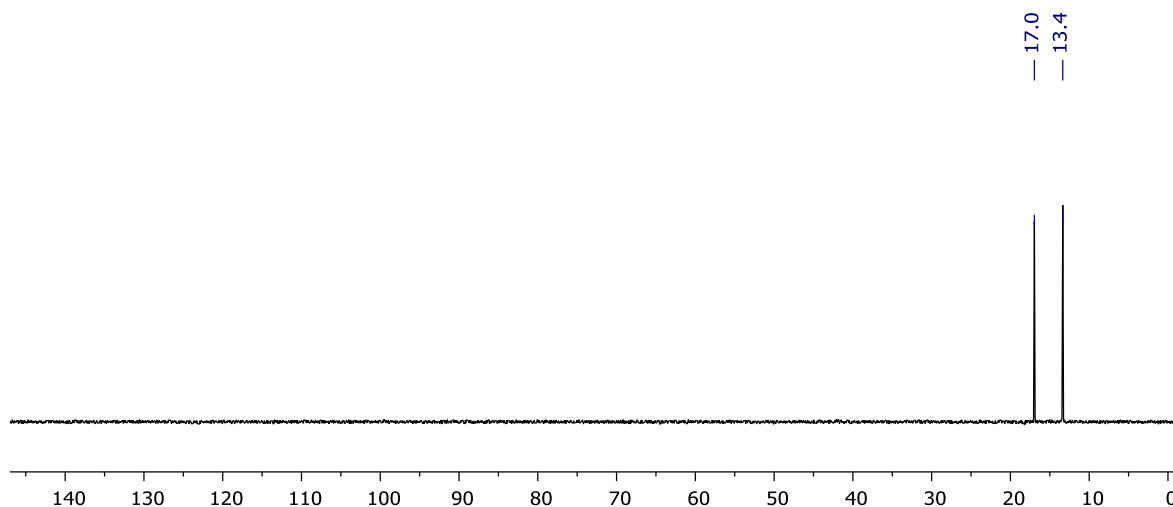


Figure S3. $^{31}\text{P}\{^1\text{H}\}$ NMR spectrum of **1** (DFB, 162 MHz).

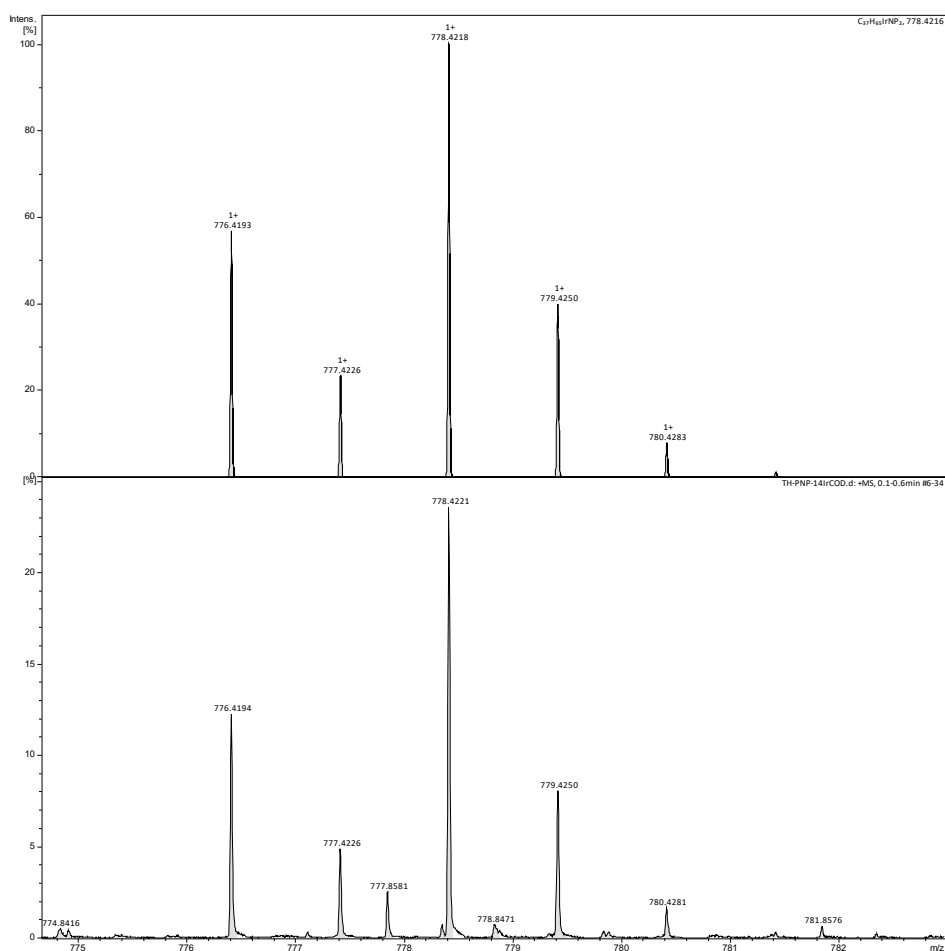


Figure S4. HR ESI-MS of 1.

2 NMR scale reaction of 1 with dihydrogen

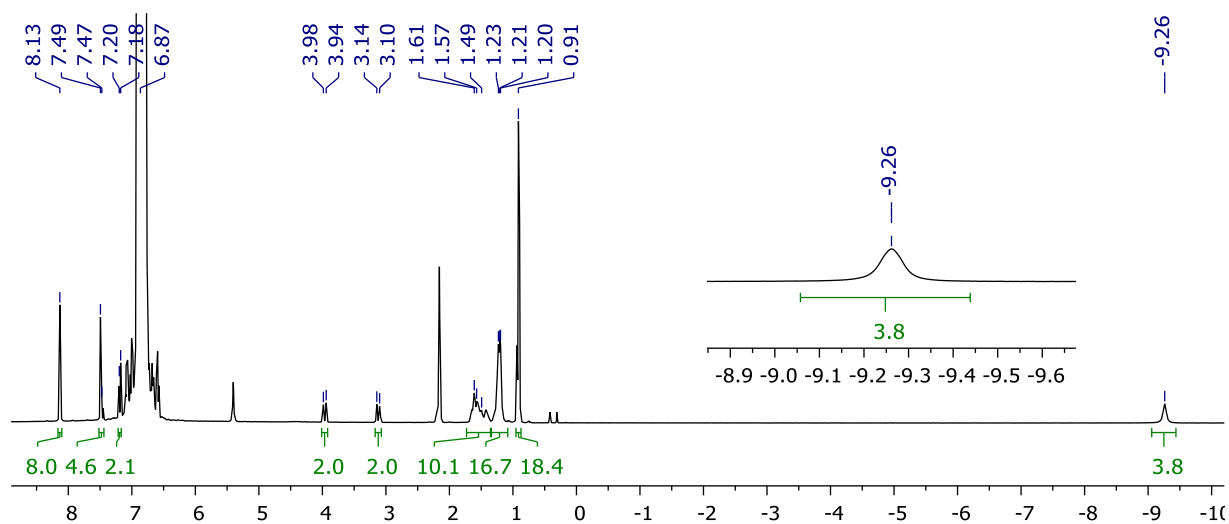


Figure S5. ^1H NMR spectrum showing formation of 4 (DFB, 400 MHz).

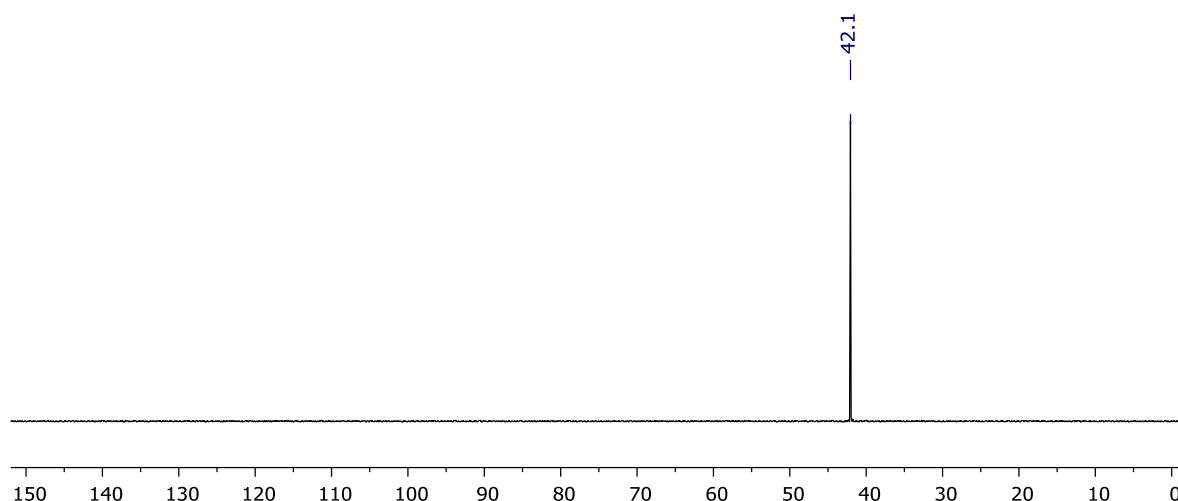


Figure S6. $^{31}\text{P}\{^1\text{H}\}$ NMR spectrum showing formation of **4** (DFB, 162 MHz).

3 Preparation of $[\text{Ir}(\text{PNP-14})(\text{biph})][\text{BAR}^{\text{F}}_4]$ (**2**)

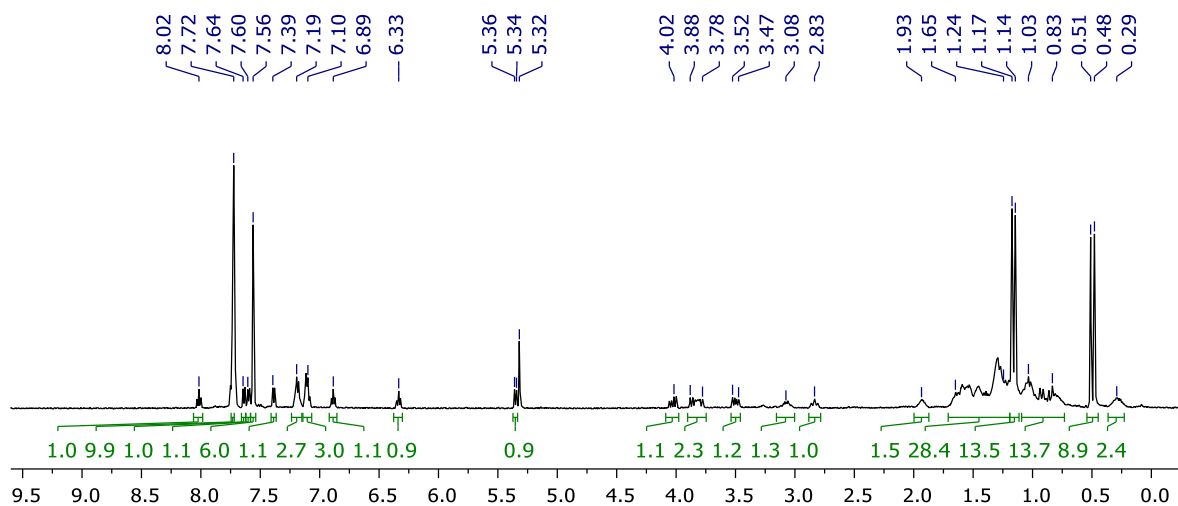


Figure S7. ^1H NMR spectrum of **2** (DFB, 500 MHz).

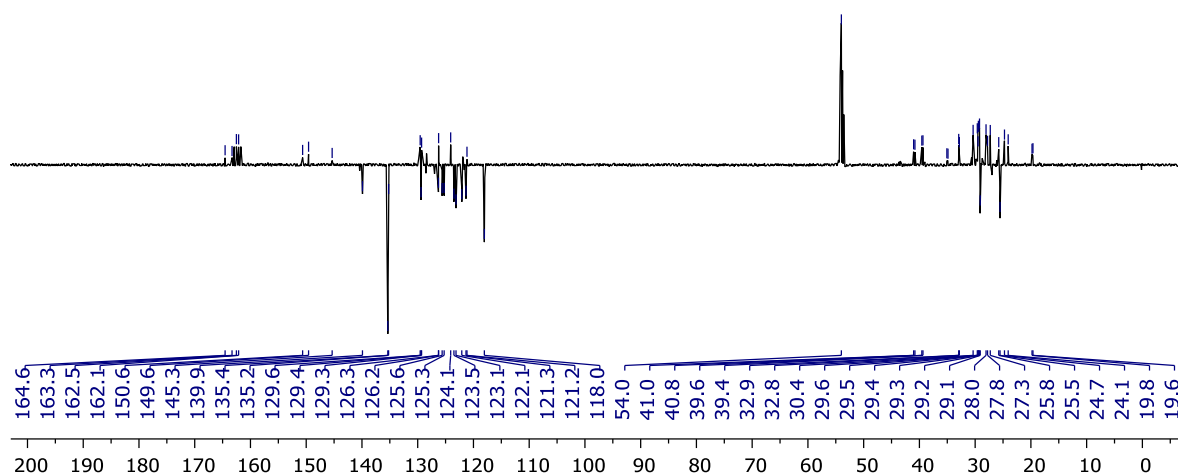


Figure S8. $^{13}\text{C}\{^1\text{H}\}$ APT NMR spectrum of **2** (DFB, 126 MHz).

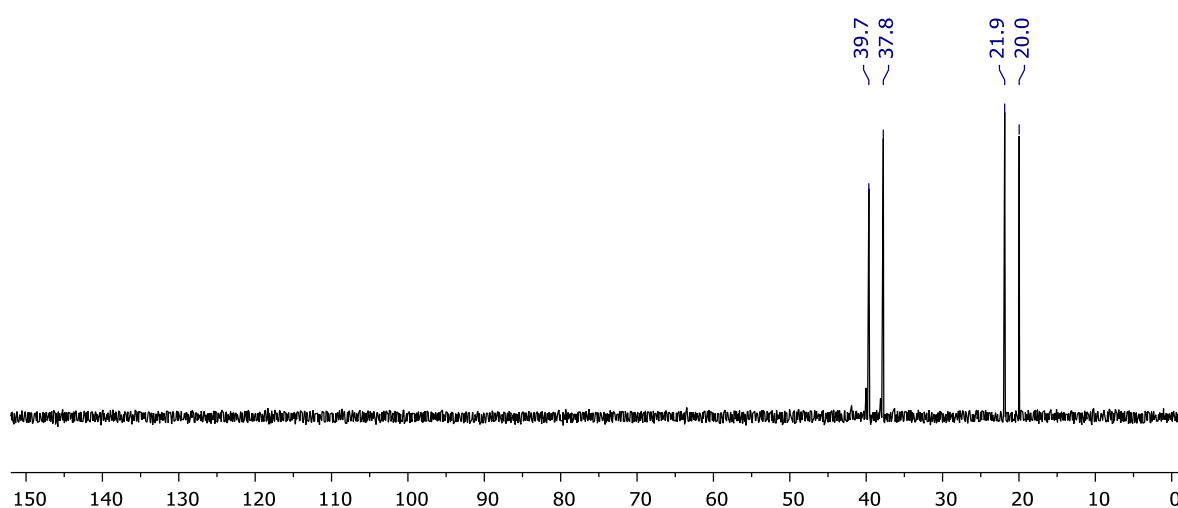


Figure S9. $^{31}\text{P}\{^1\text{H}\}$ NMR spectrum of **2** (DFB, 162 MHz).

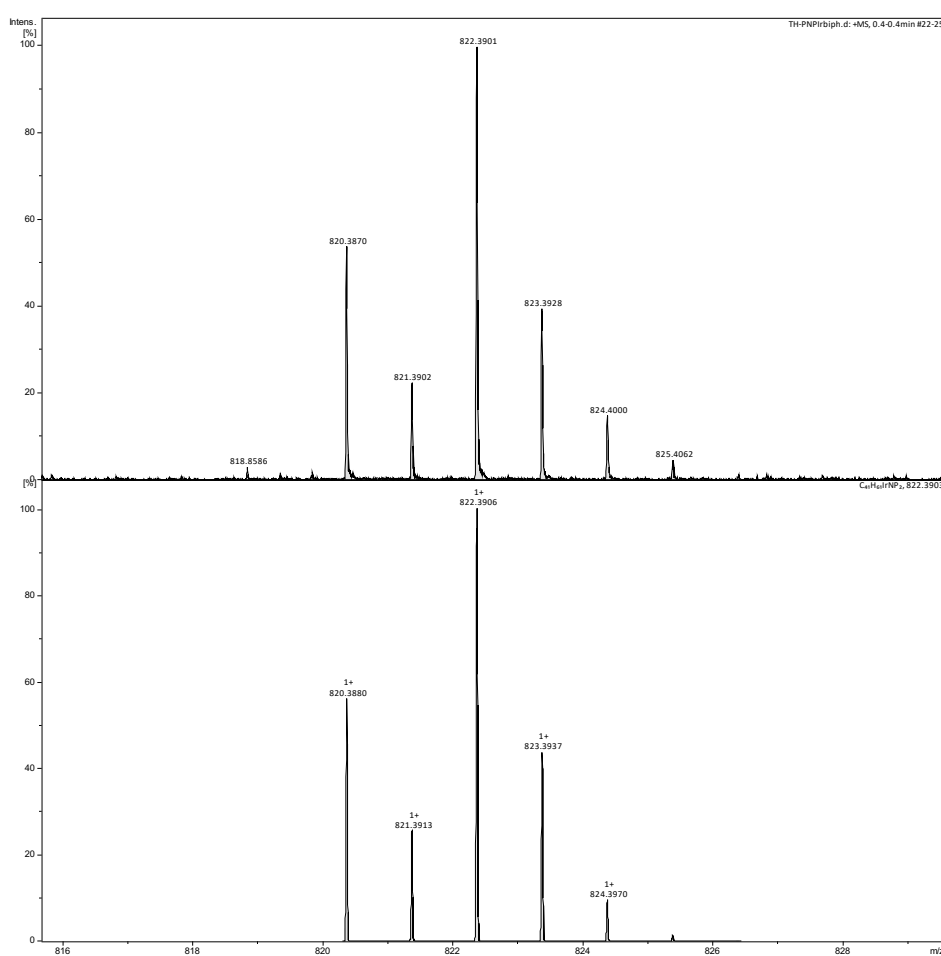


Figure S10. HR ESI-MS of **2**.

4 NMR scale reactions of 2

4.1 Synthesis of $[\text{Ir}(\text{PNP-14})(2\text{-biphenyl})\text{H}][\text{BAr}^{\text{F}}_4]$ (**3**)

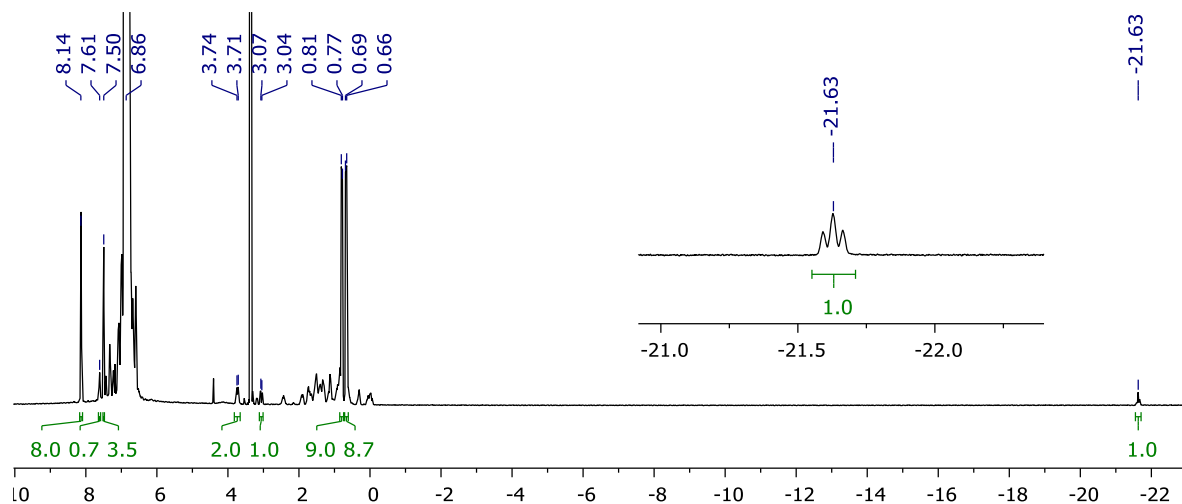


Figure S11. ^1H NMR spectrum showing formation of **3** (DFB, 400 MHz).

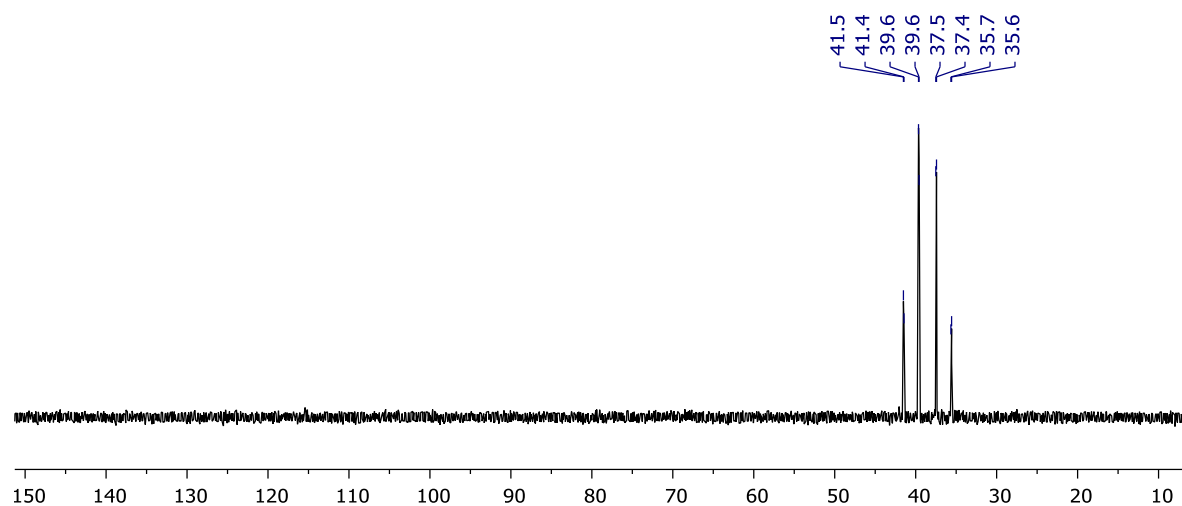


Figure S12. $^{31}\text{P}\{^1\text{H}\}$ NMR spectrum showing formation of **3** (DFB, 162 MHz).

4.2 Synthesis of $[\text{Ir}(\text{PNP-14})\text{H}_2(\text{H}_2)][\text{BAr}^{\text{F}}_4]$ (**4**)

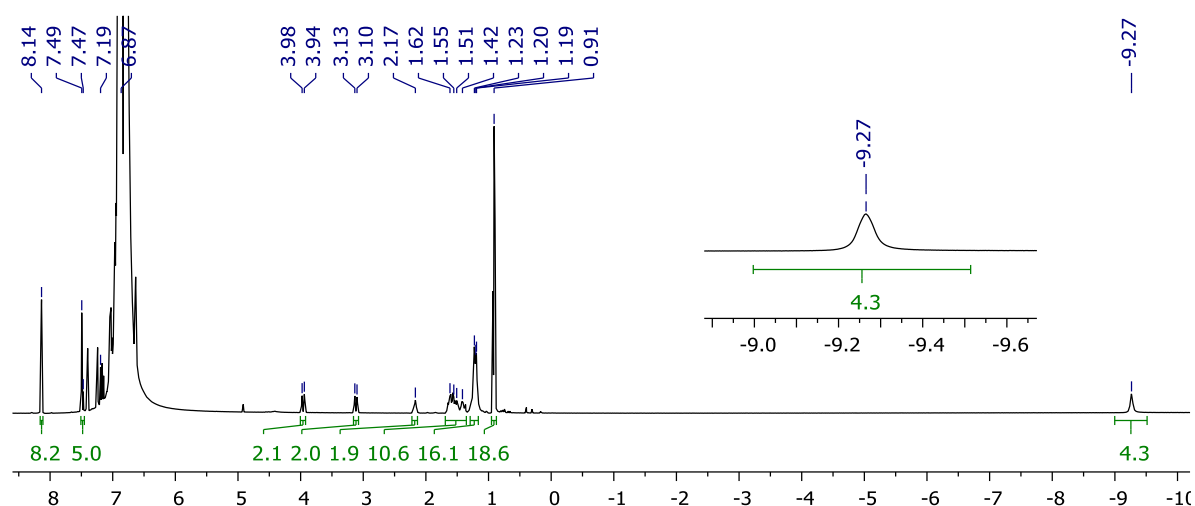


Figure S13. ^1H NMR spectrum showing formation of **4** (DFB, 500 MHz).

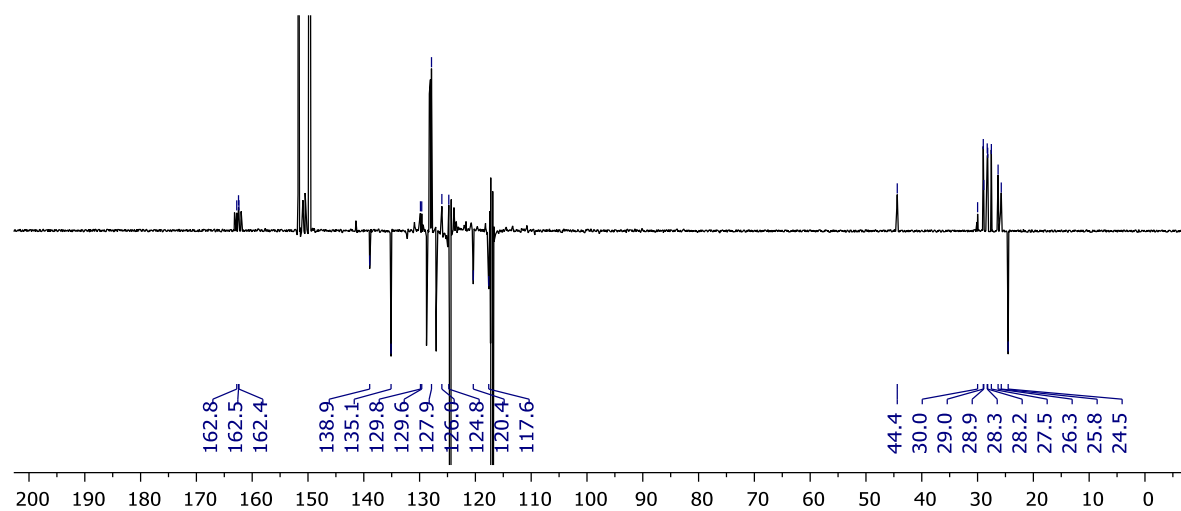


Figure S14. $^{13}\text{C}\{^1\text{H}\}$ APT NMR spectrum showing formation of **4** (DFB, 126 MHz).

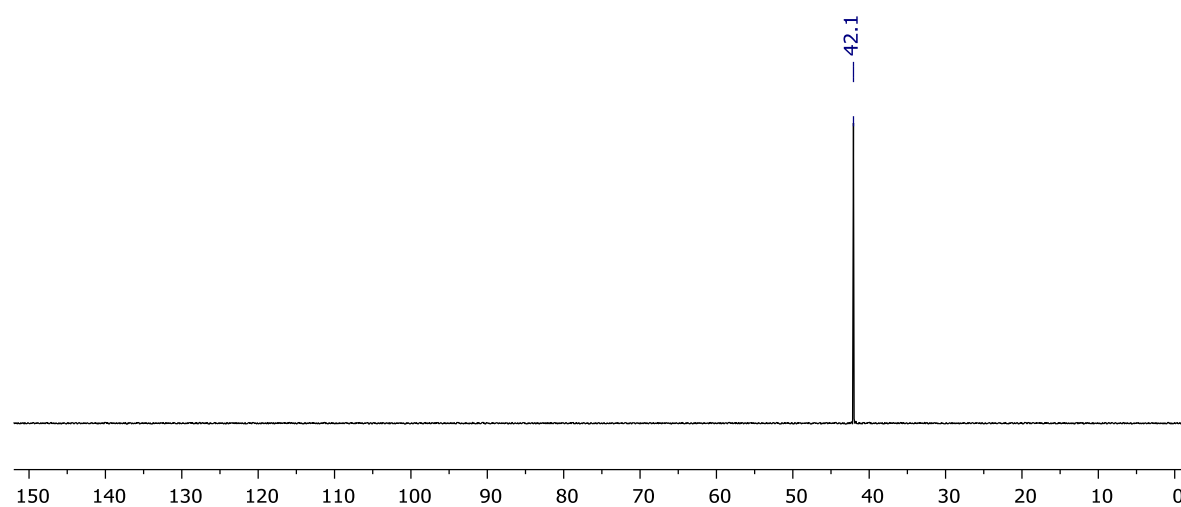


Figure S15. $^{31}\text{P}\{^1\text{H}\}$ NMR spectrum showing formation of **4** (DFB, 162 MHz).

4.3 Synthesis of $[\text{Ir}(\text{PNP-14})\text{H}_2(\text{C}_2\text{H}_4)][\text{BAr}^{\text{F}}_4]$ (**5**)

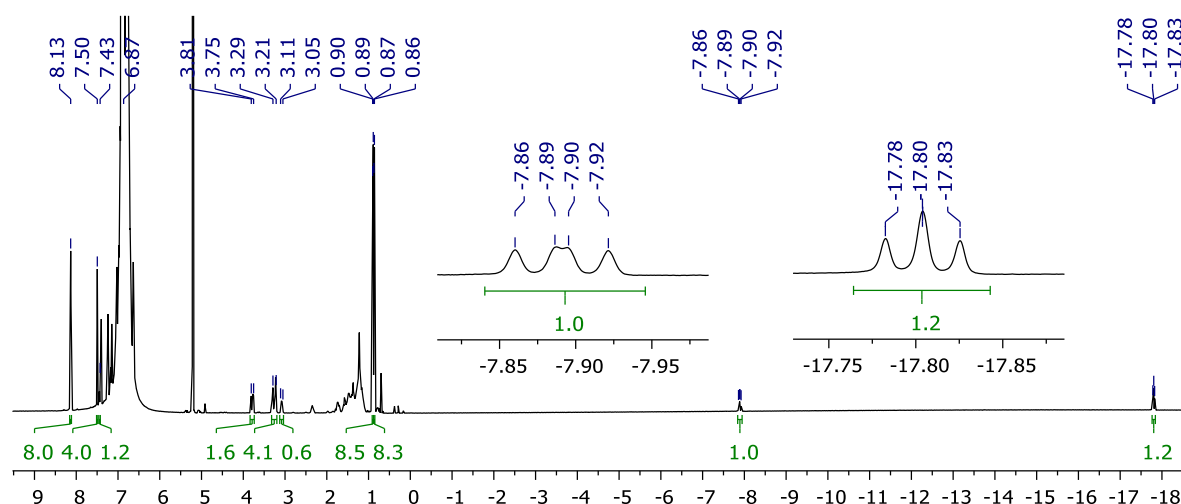


Figure S16. ¹H NMR spectrum showing formation of **5** (DFB, 500 MHz).

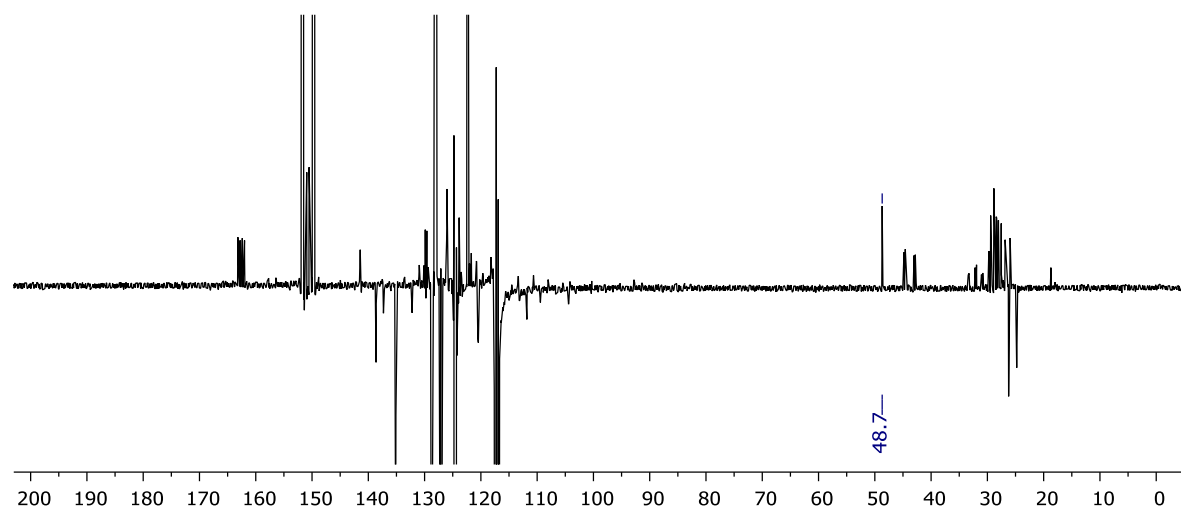


Figure S17. ¹³C{¹H} APT NMR spectrum showing formation of **5** (DFB, 126 MHz).

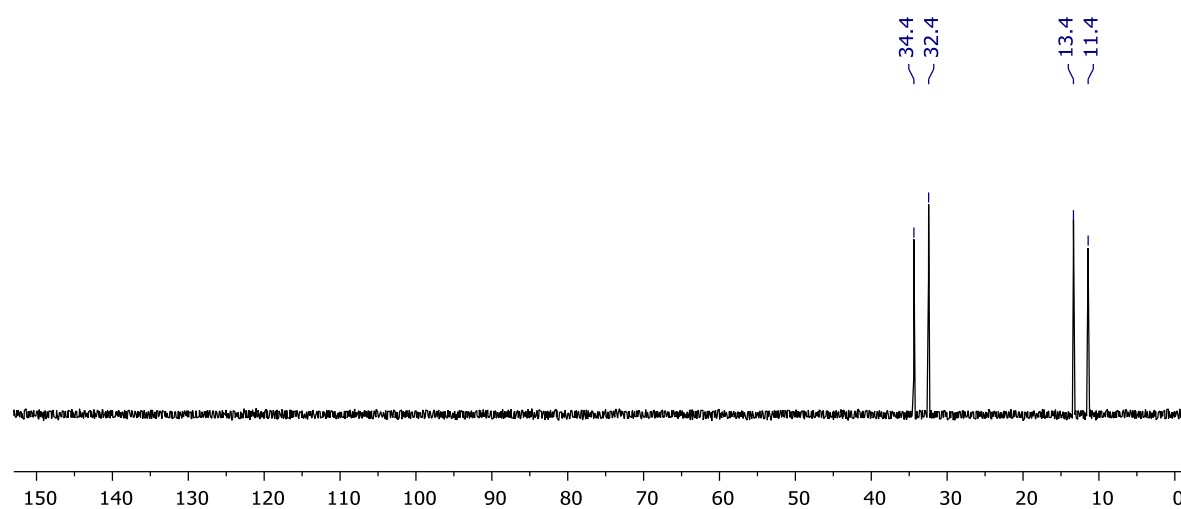


Figure S18. ³¹P{¹H} NMR spectrum showing formation of **5** (DFB, 162 MHz).

4.4 Synthesis of $[\text{Ir}(\text{PNP-14})(\text{C}_2\text{H}_4)_2][\text{BAR}^{\text{F}}_4]$ (**6**)

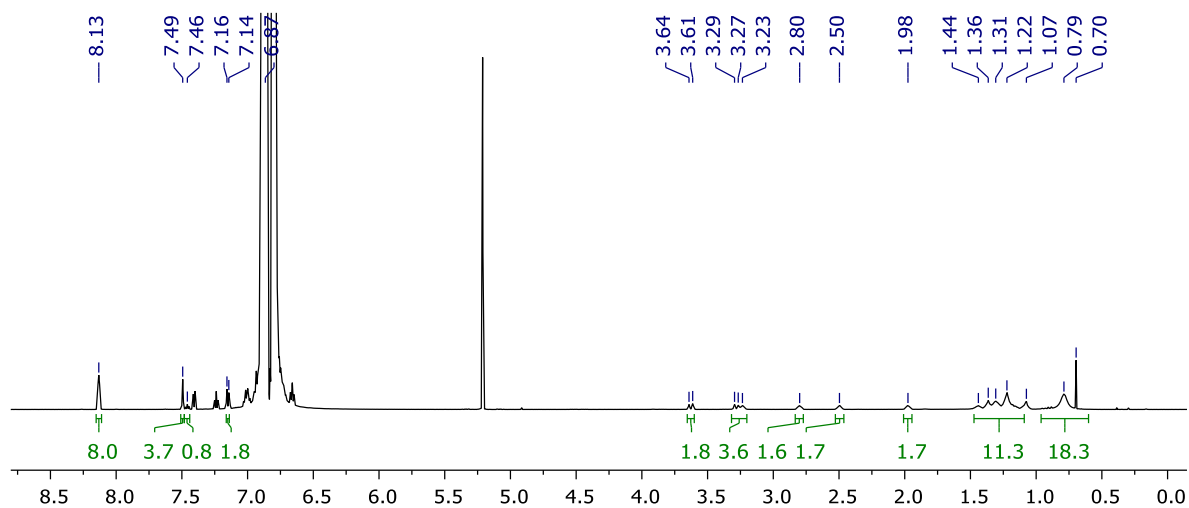


Figure S19. ^1H NMR spectrum showing formation of **6** (DFB, 600 MHz).

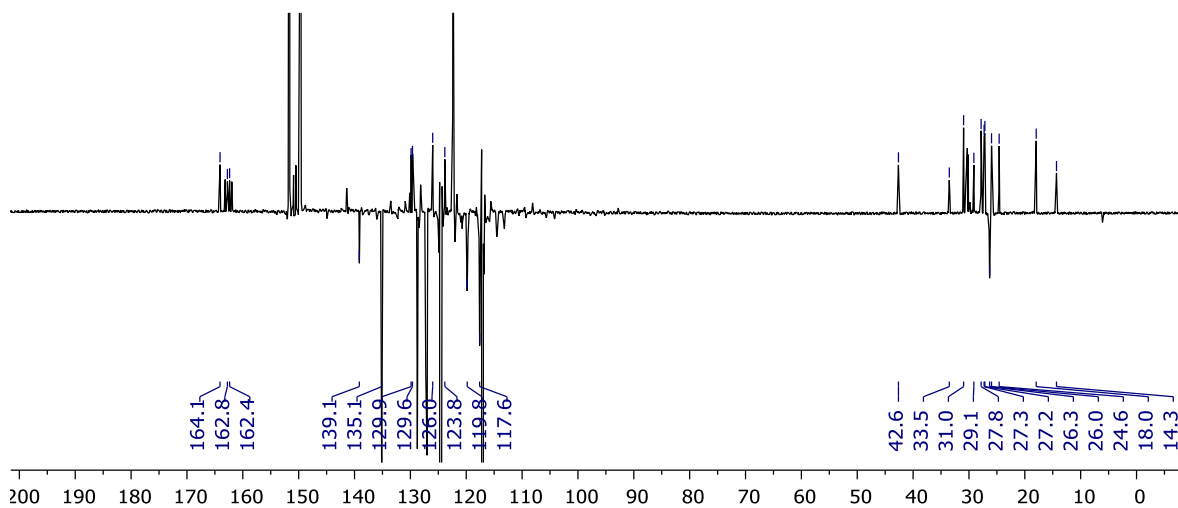


Figure S20. $^{13}\text{C}\{^1\text{H}\}$ APT NMR spectrum showing formation of **6** (DFB, 126 MHz).

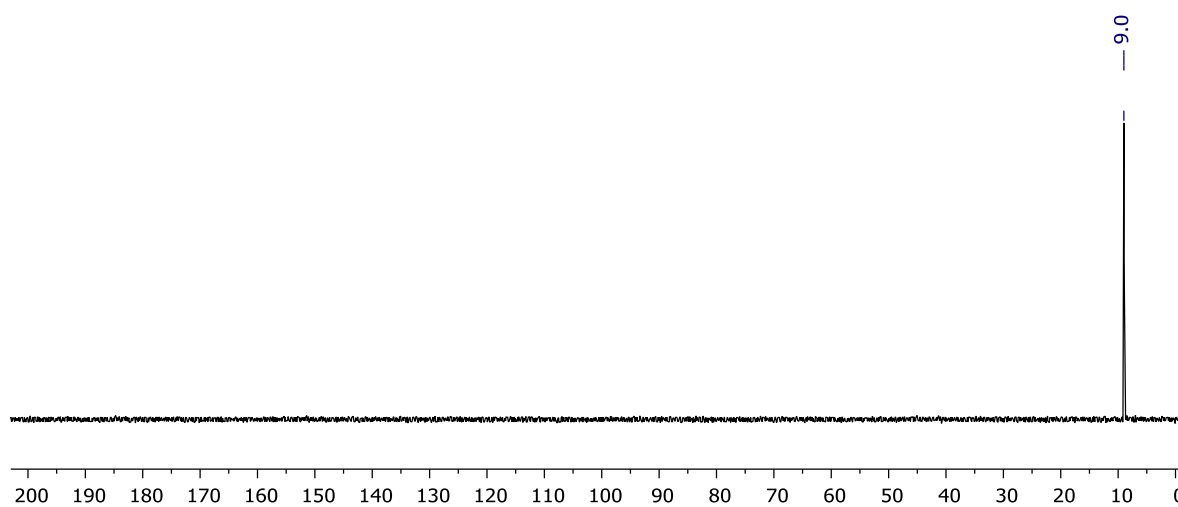


Figure S21. $^{31}\text{P}\{^1\text{H}\}$ NMR spectrum showing formation of **6** (DFB, 162 MHz).

4.5 Synthesis and isolation of $[\text{Ir}(\text{PNP-14})(\text{CO})][\text{BAR}^{\text{F}}_4]$ (**8**)

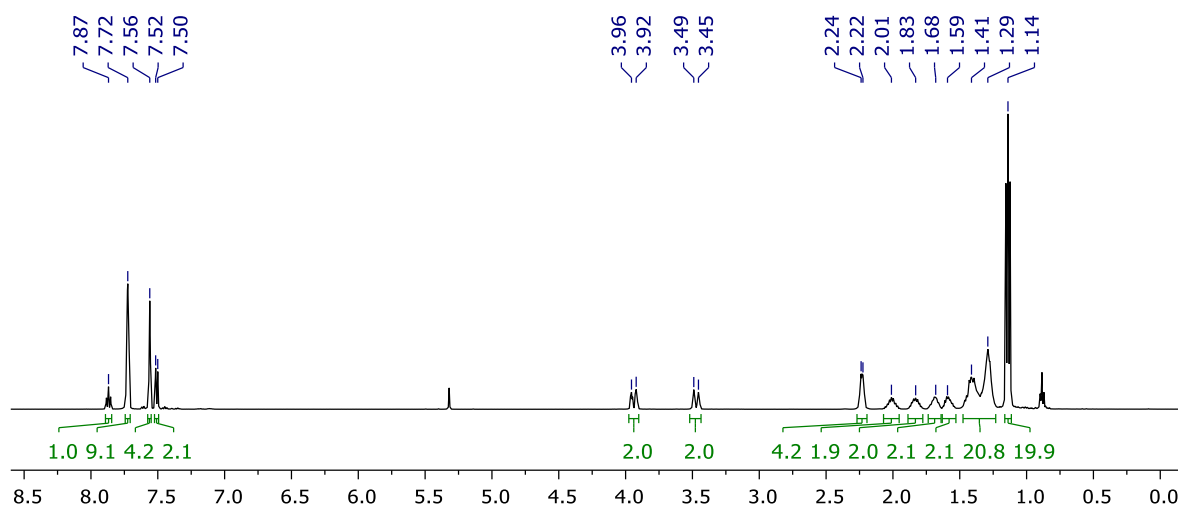


Figure S22. ^1H NMR spectrum of isolated **8** (CD_2Cl_2 , 500 MHz).

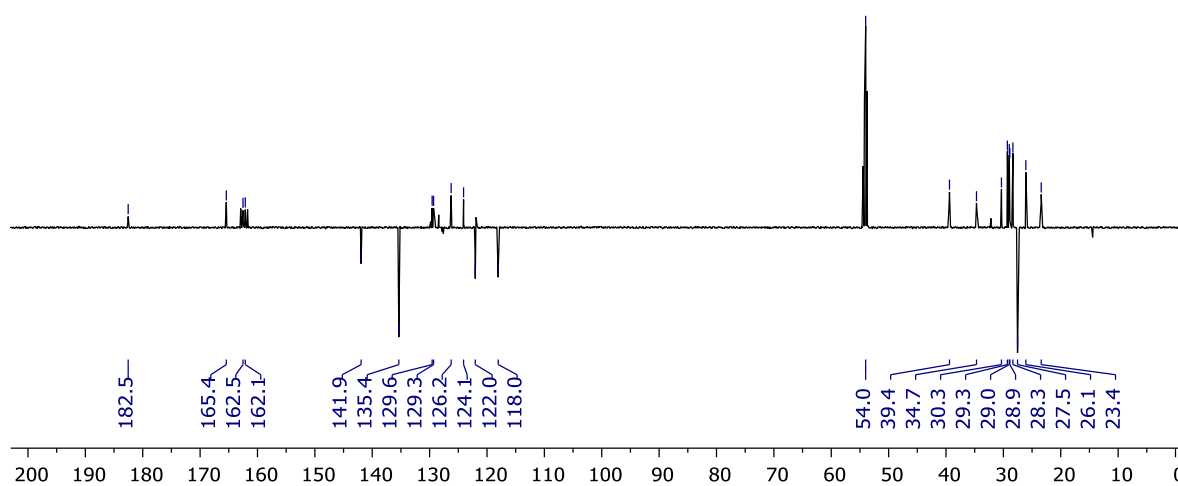


Figure S23. $^{13}\text{C}\{^1\text{H}\}$ APT NMR spectrum of isolated **8** (CD_2Cl_2 , 126 MHz).

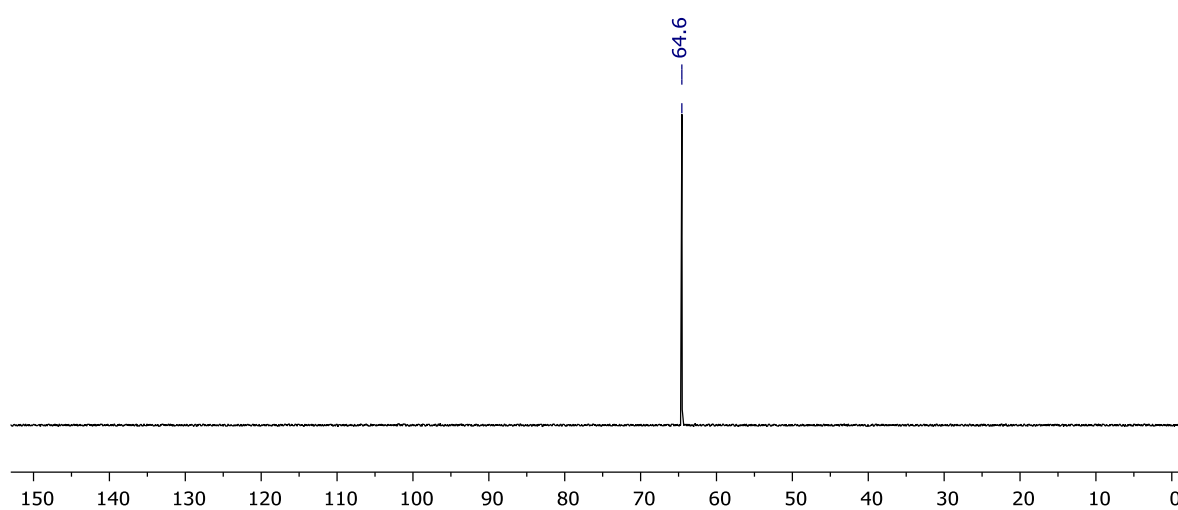


Figure S24. $^{31}\text{P}\{^1\text{H}\}$ NMR spectrum of isolated **8** (CD_2Cl_2 , 162 MHz).

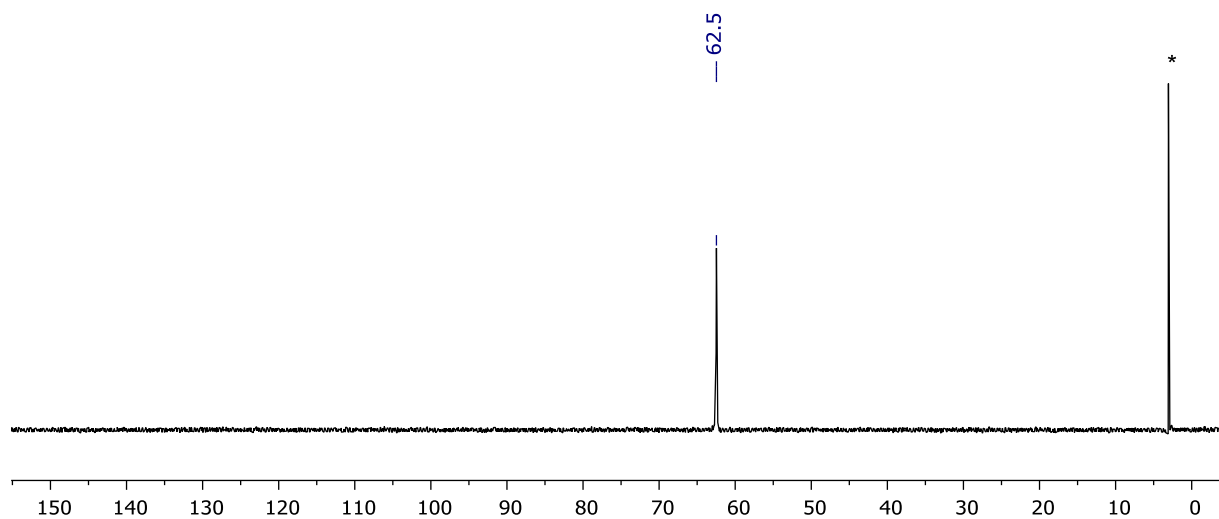


Figure S25. $^{31}\text{P}\{^1\text{H}\}$ NMR spectrum of isolated **8** (DFB, 162 MHz). * = internal reference.

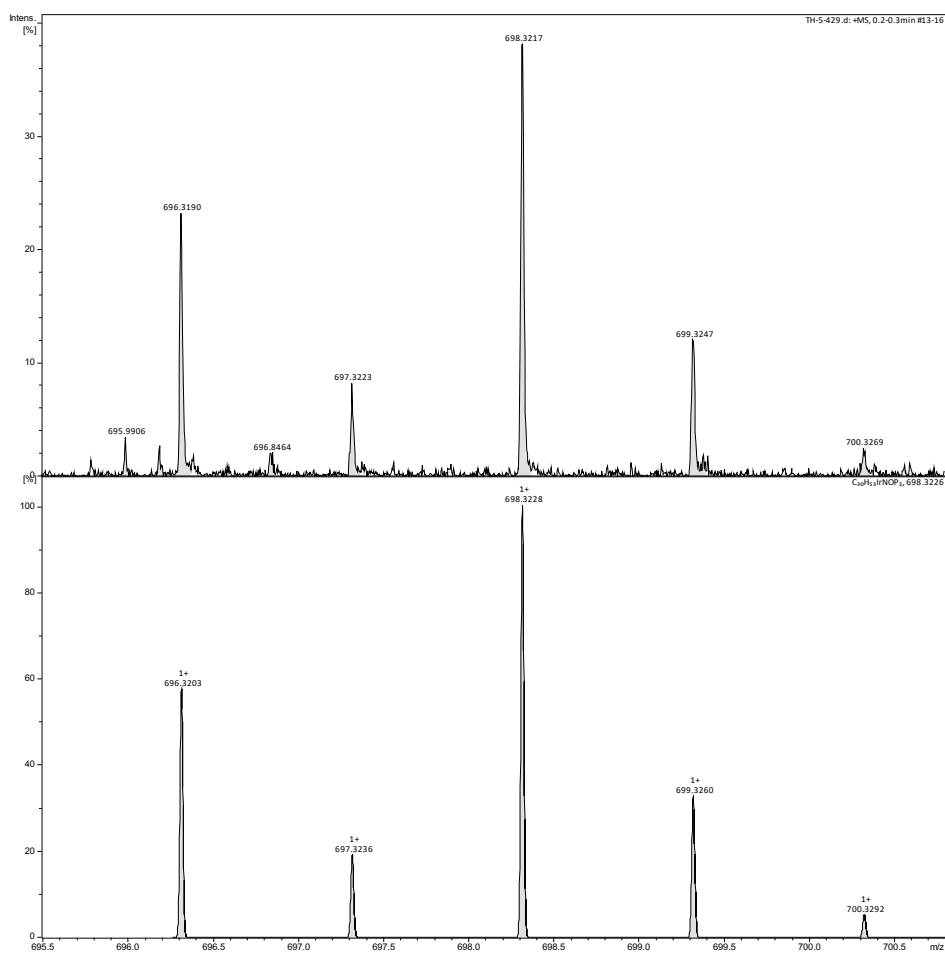


Figure S26. HR ESI-MS of isolated **8**.

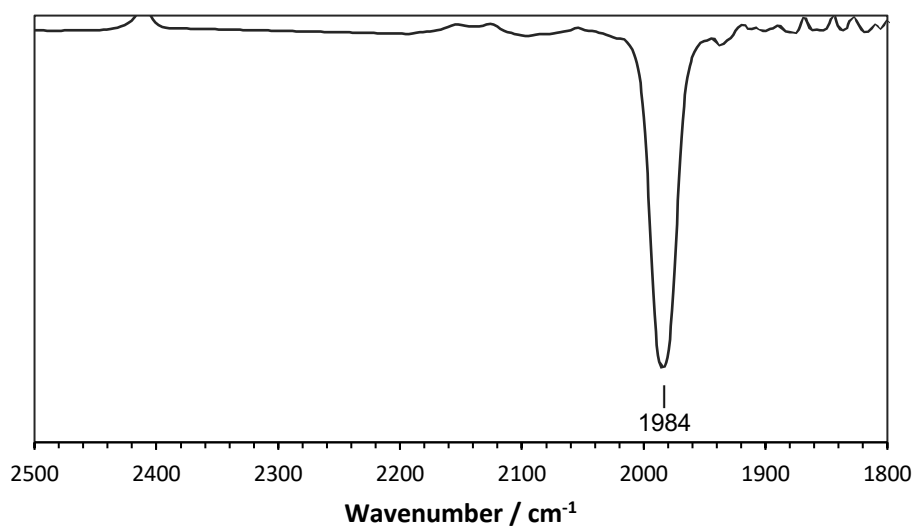


Figure S27. IR spectrum of isolated **8** recorded in CH₂Cl₂.

5 NMR scale reaction of [Ir(PNP-*t*Bu)(biph)][BAr^F₄] (**II**) with dihydrogen

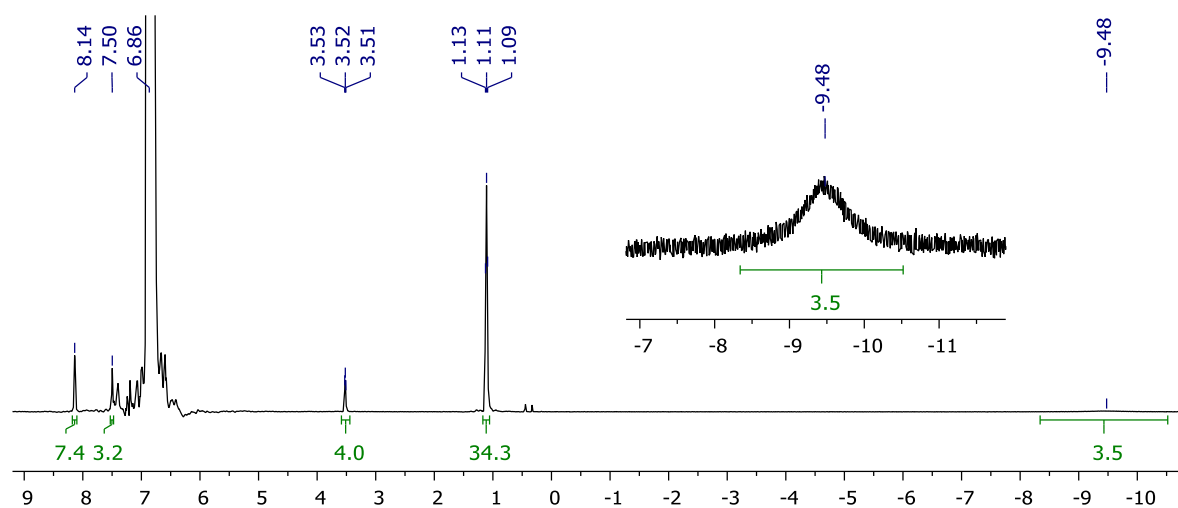


Figure S28. ¹H NMR spectrum showing formation of [Ir(PNP-*t*Bu)H₂(H₂)] [BAr^F₄] (DFB, 400 MHz).

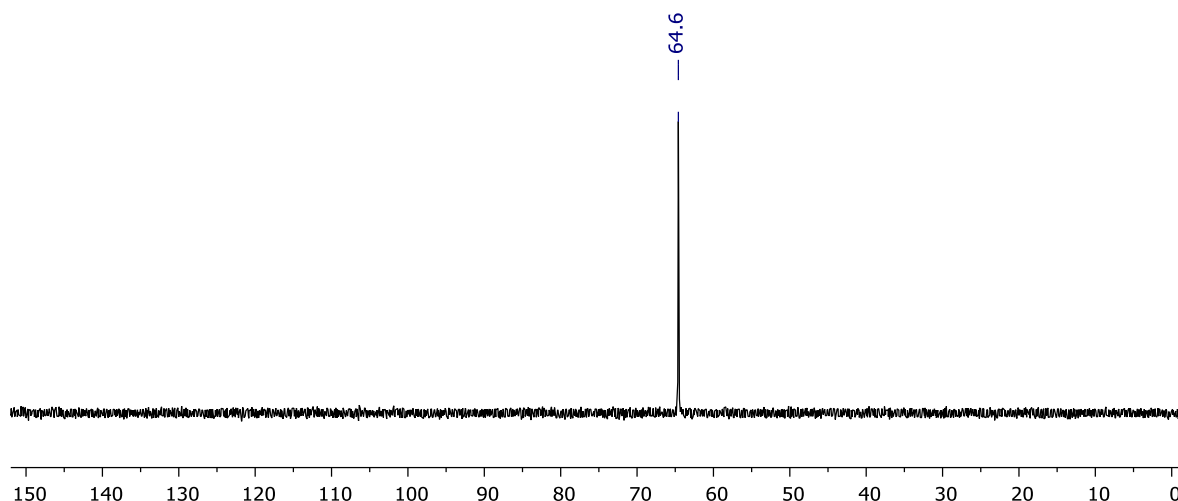


Figure S29. $^{31}\text{P}\{^1\text{H}\}$ NMR spectrum showing formation of $[\text{Ir}(\text{PNP-}t\text{Bu})\text{H}_2(\text{H}_2)][\text{BAR}^{\text{F}}_4]$ (DFB, 162 MHz).

6 Preparation of $[\text{Ir}(\text{PNP-14}^*)\text{H}][\text{BAR}^{\text{F}}_4]$ (7)

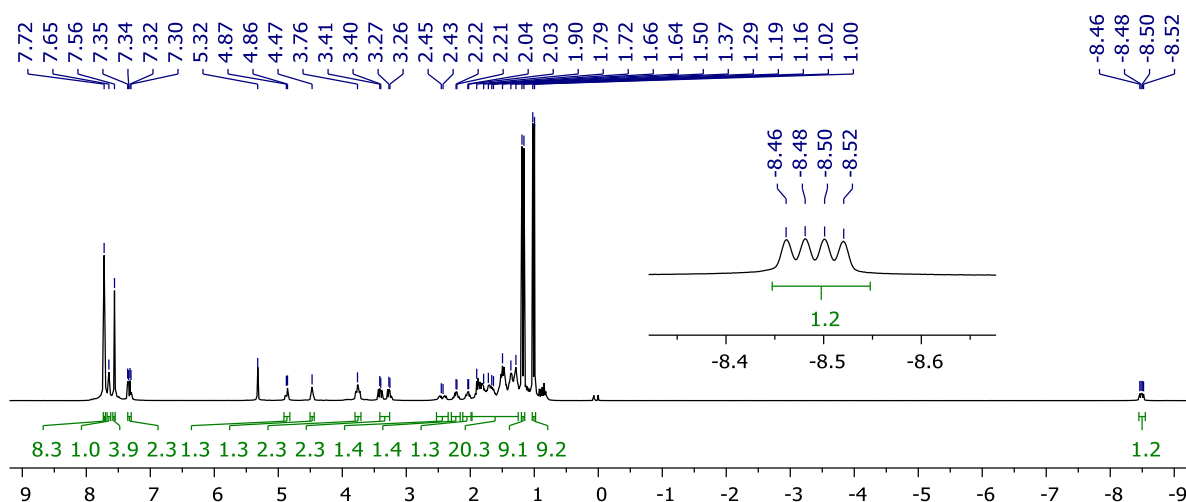


Figure S30. ^1H NMR spectrum of **7** (CD_2Cl_2 , 500 MHz).

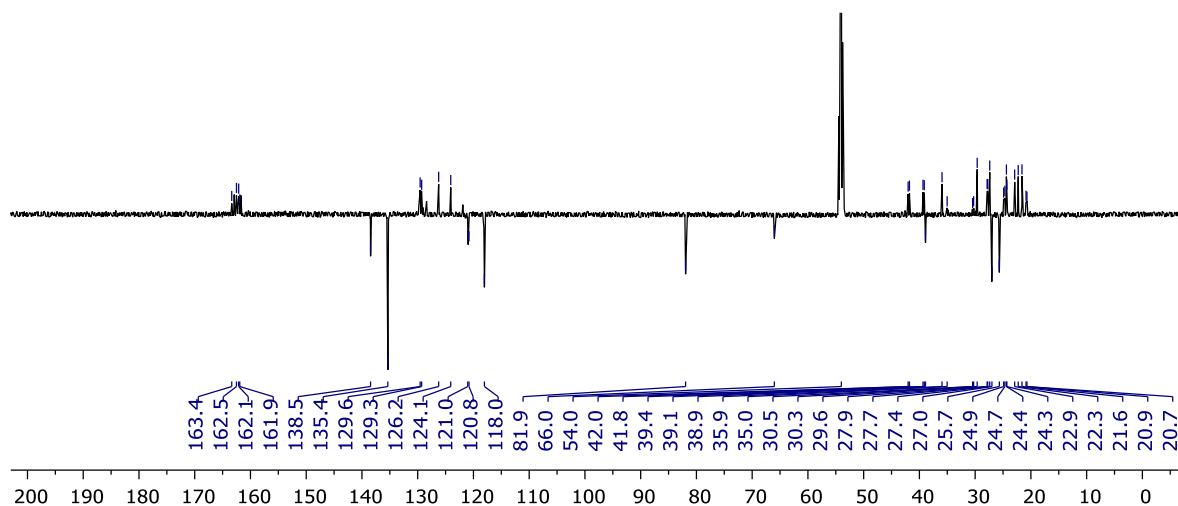


Figure S31. $^{13}\text{C}\{^1\text{H}\}$ APT NMR spectrum of **7** (CD_2Cl_2 , 126 MHz).

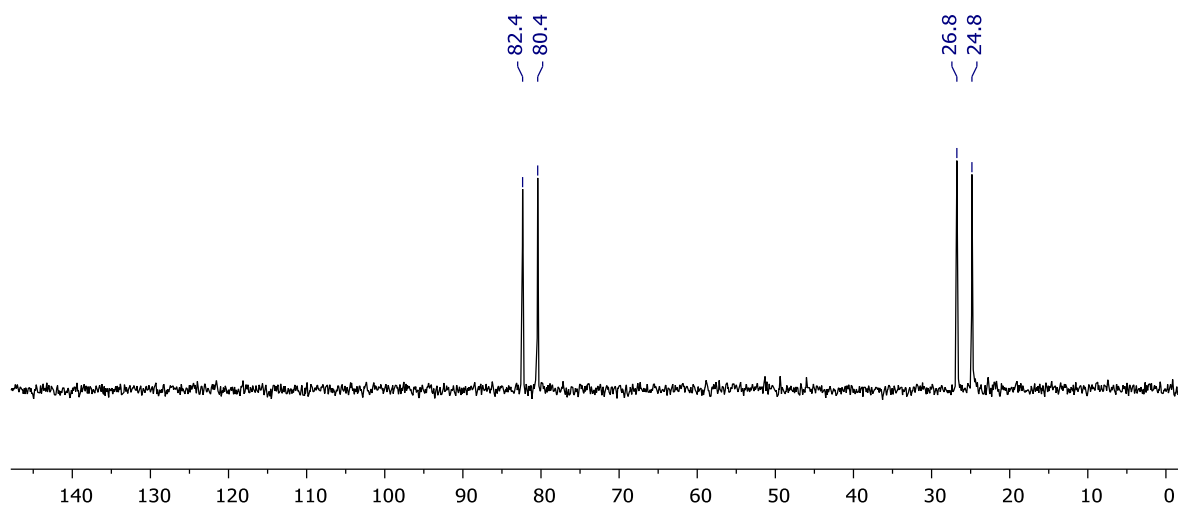


Figure S32. $^{31}\text{P}\{^1\text{H}\}$ NMR spectrum of **7** (CD_2Cl_2 , 162 MHz).

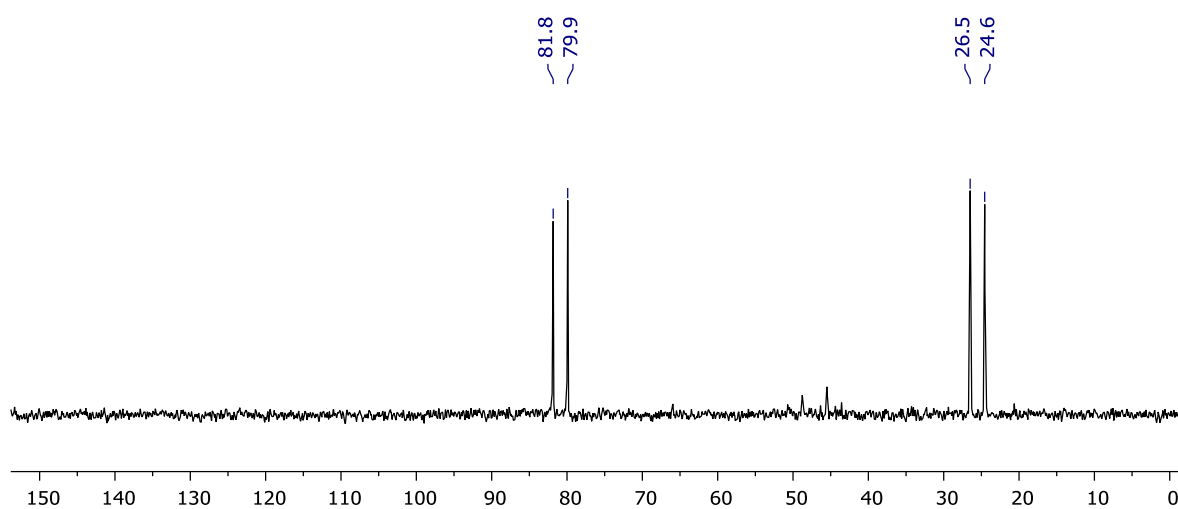


Figure S33. $^{31}\text{P}\{^1\text{H}\}$ NMR spectrum of **7** (DFB, 162 MHz).

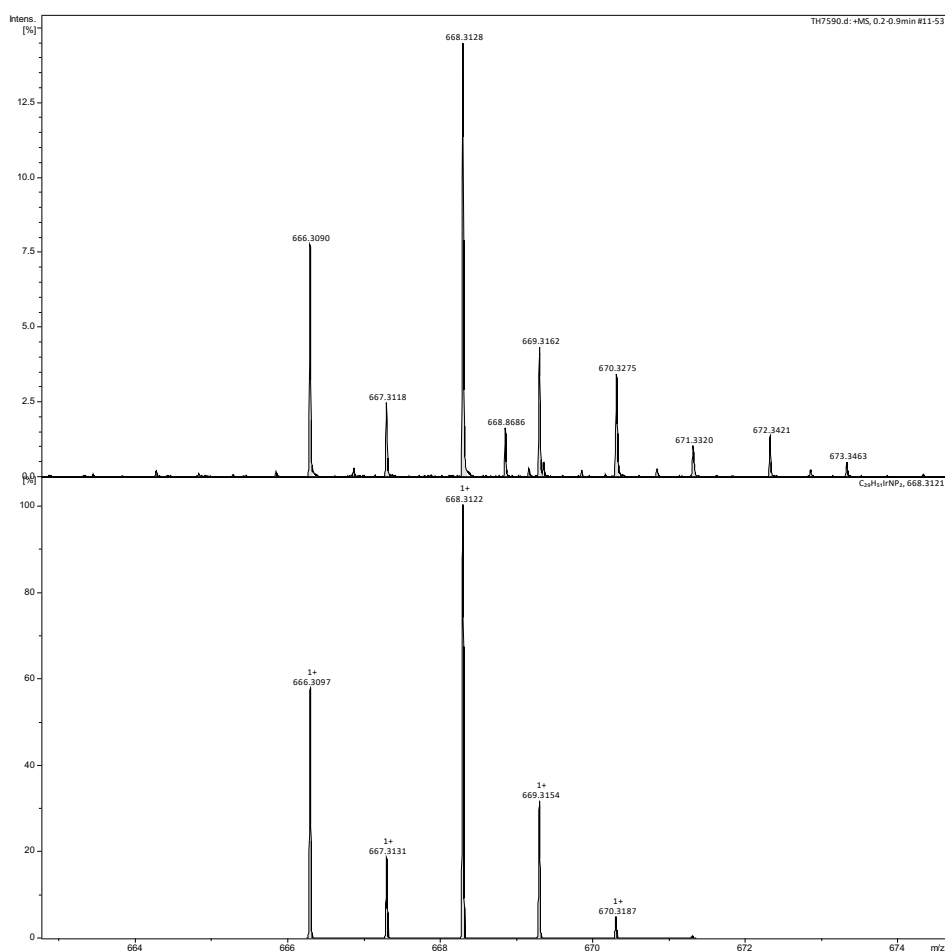


Figure S34. HR ESI-MS of **7**.

7 NMR scale reaction of **7** with dihydrogen

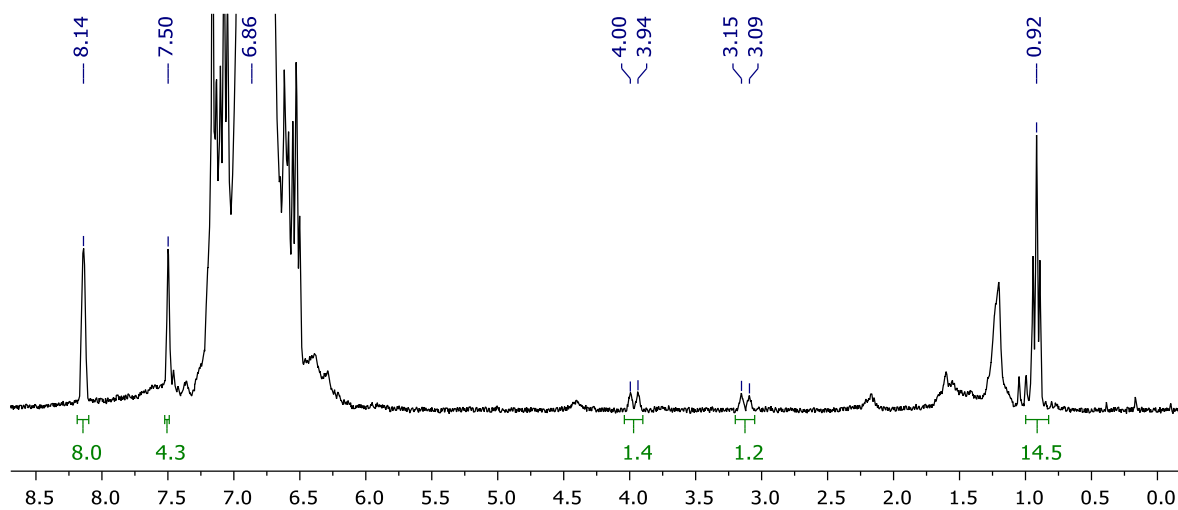


Figure S35. ^1H NMR spectrum showing formation of **4** (DFB, 300 MHz).

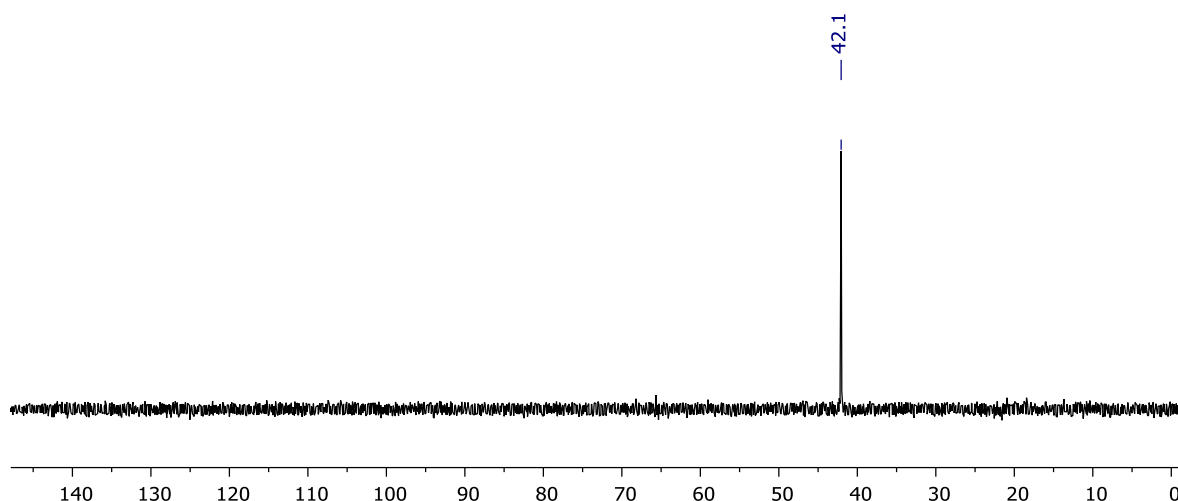


Figure S36. $^{31}\text{P}\{^1\text{H}\}$ NMR spectrum showing formation of **4** (DFB, 121 MHz).

8 Catalytic homocoupling of 3,3-dimethylbutyne promoted by **1**

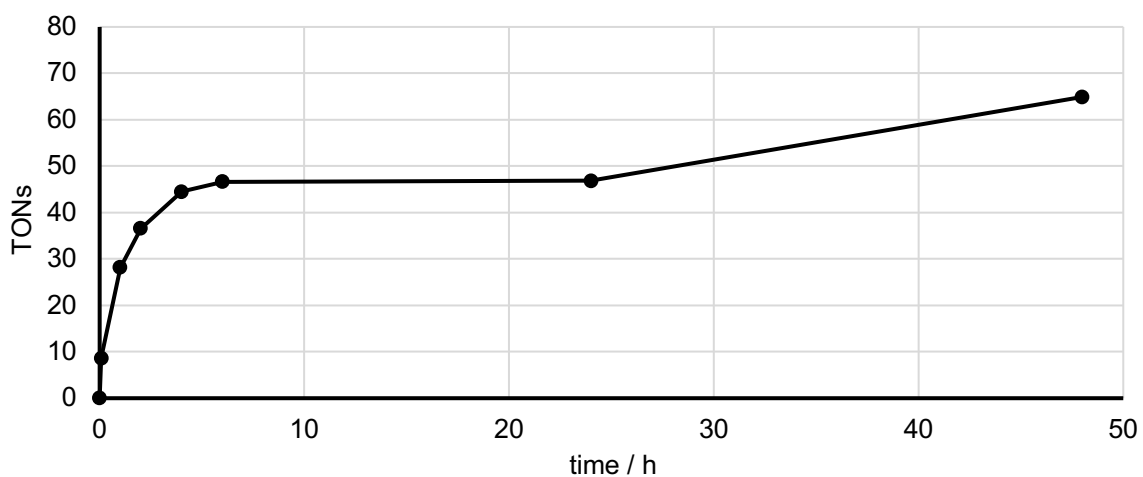


Figure S37. Catalytic homocoupling of 3,3-dimethylbutyne promoted by **1** (1 mol%, initially) and producing Z - $t\text{BuC}\equiv\text{CCHCH}t\text{Bu}$. Full experimental details provided in the manuscript. An additional 50 equivalents of substrate were added to the reaction mixture after 24 h.

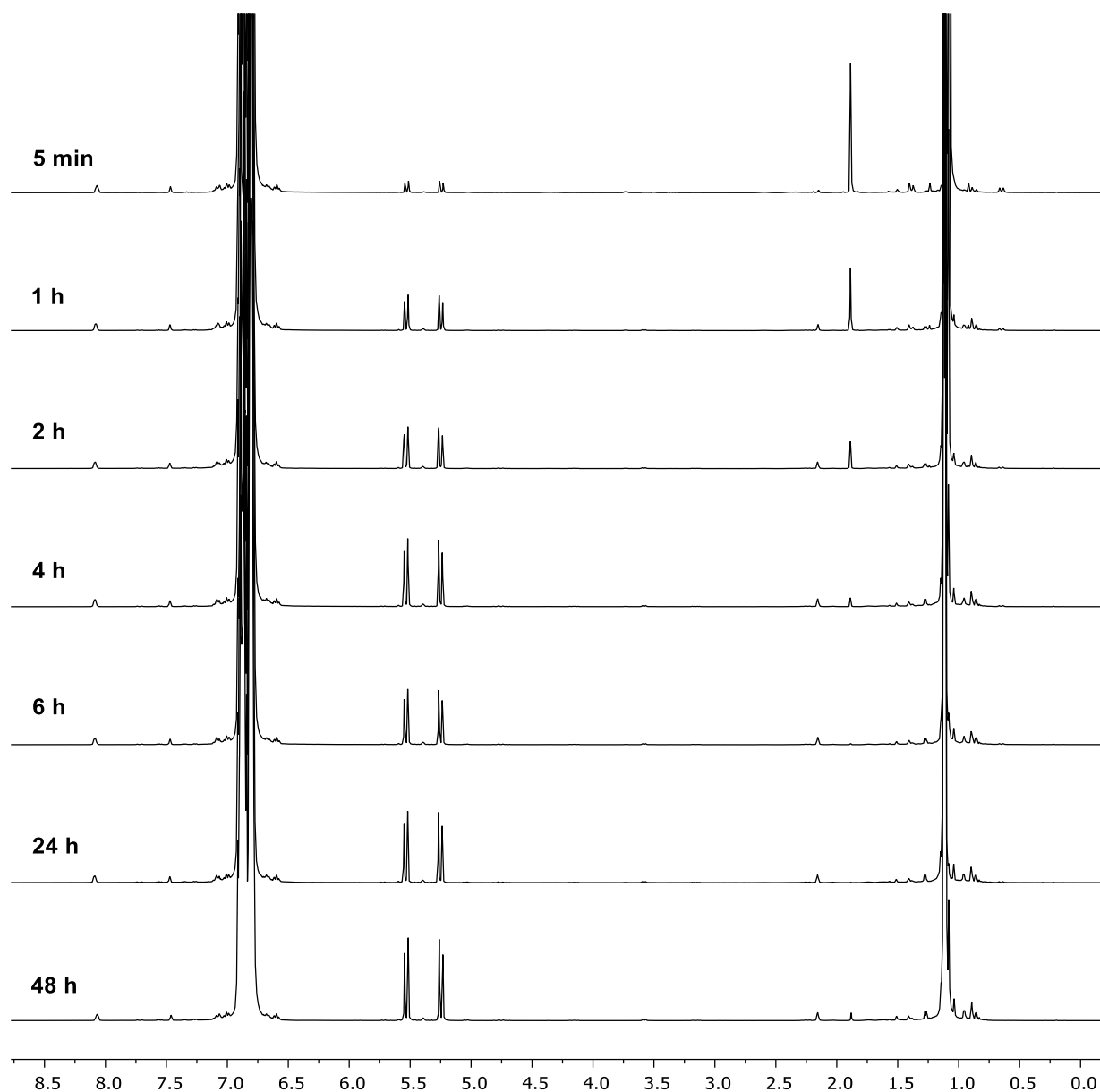


Figure S38. ¹H NMR spectra (DFB, 400 MHz) collected during the homocoupling of 3,3-dimethylbutyne promoted by **1** (1 mol%, initially) and producing *Z*-*t*BuC≡CCHCH*t*Bu. Full experimental details provided in the manuscript. An additional 50 equivalents of substrate were added to the reaction mixture after 24 h.

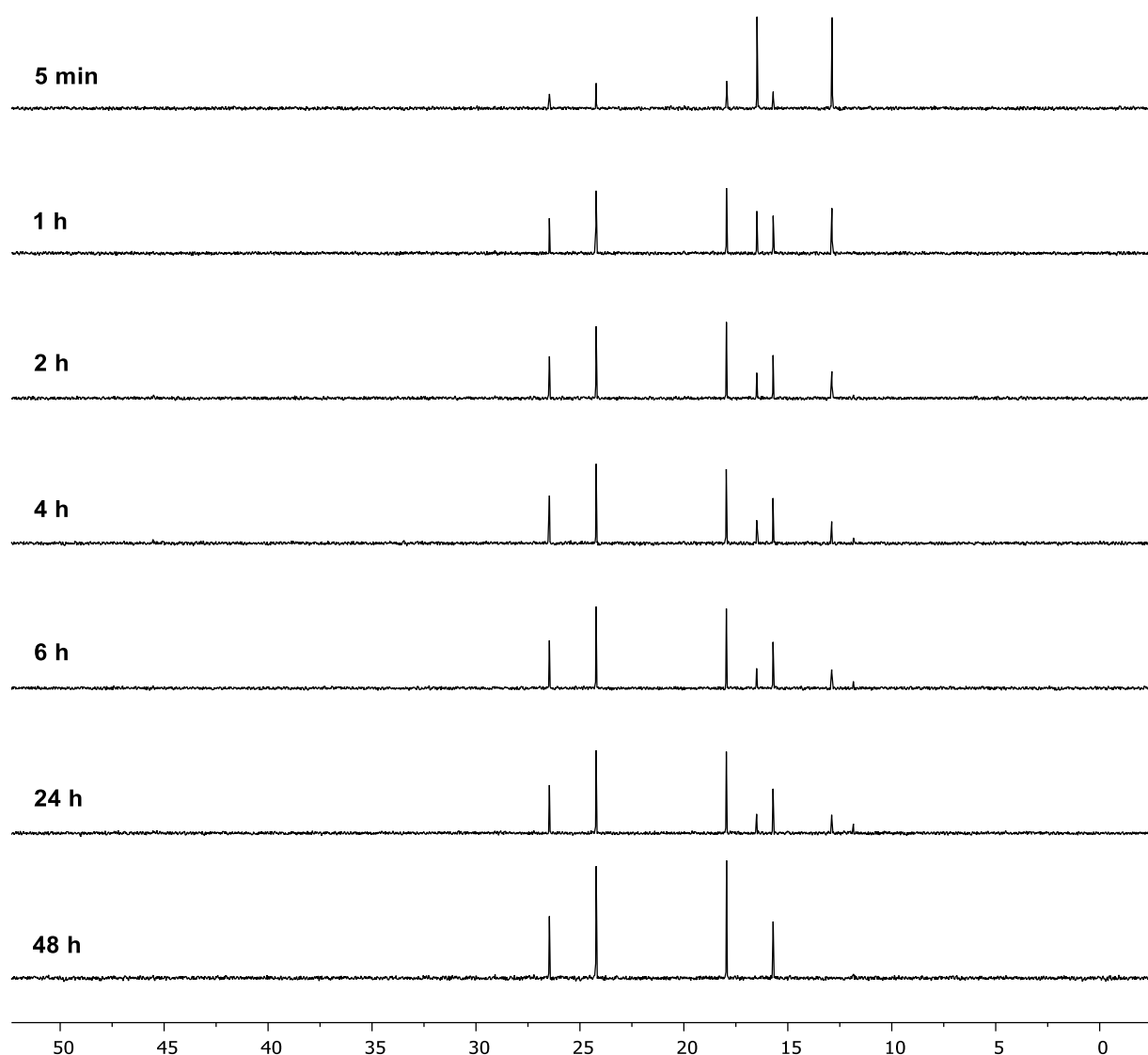


Figure S39. $^{31}\text{P}\{^1\text{H}\}$ NMR spectra (DFB, 162 MHz) collected during the homocoupling of 3,3-dimethylbutyne promoted by **1** (1 mol%, initially) and producing Z - $t\text{BuC}\equiv\text{CCHCH}t\text{Bu}$. Full experimental details provided in the manuscript. An additional 50 equivalents of substrate were added to the reaction mixture after 24 h.

9 Catalytic homocoupling of 3,3-dimethylbutyne promoted by **6**

A solution of **6** (6.4 μmol , generated in situ) in DFB (512 μL) within a J. Young NMR tube was treated with a solution of 3,3-dimethylbutyne (79 μL , 642 μmol) and the resulting homocoupling reaction producing only $Z\text{-}t\text{BuC}\equiv\text{CCHCH}t\text{Bu}$ followed at RT *in situ* using NMR spectroscopy. The solution was mixed constantly when not in the spectrometer. After 6 h the homocoupling was complete and **10** was observed as the major organometallic species (ca. 70%).

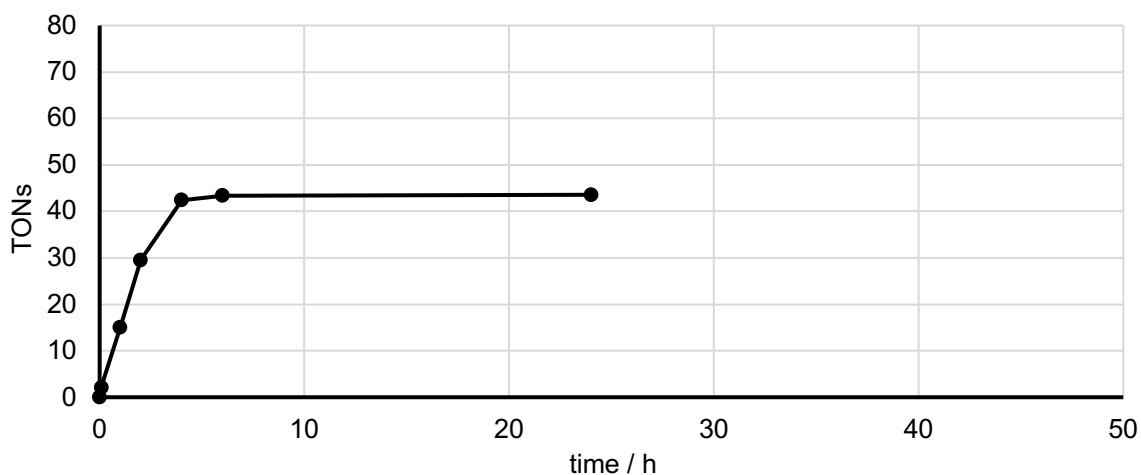


Figure S40. Catalytic homocoupling of 3,3-dimethylbutyne promoted by **6** (1 mol%) and producing $Z\text{-}t\text{BuC}\equiv\text{CCHCH}t\text{Bu}$.

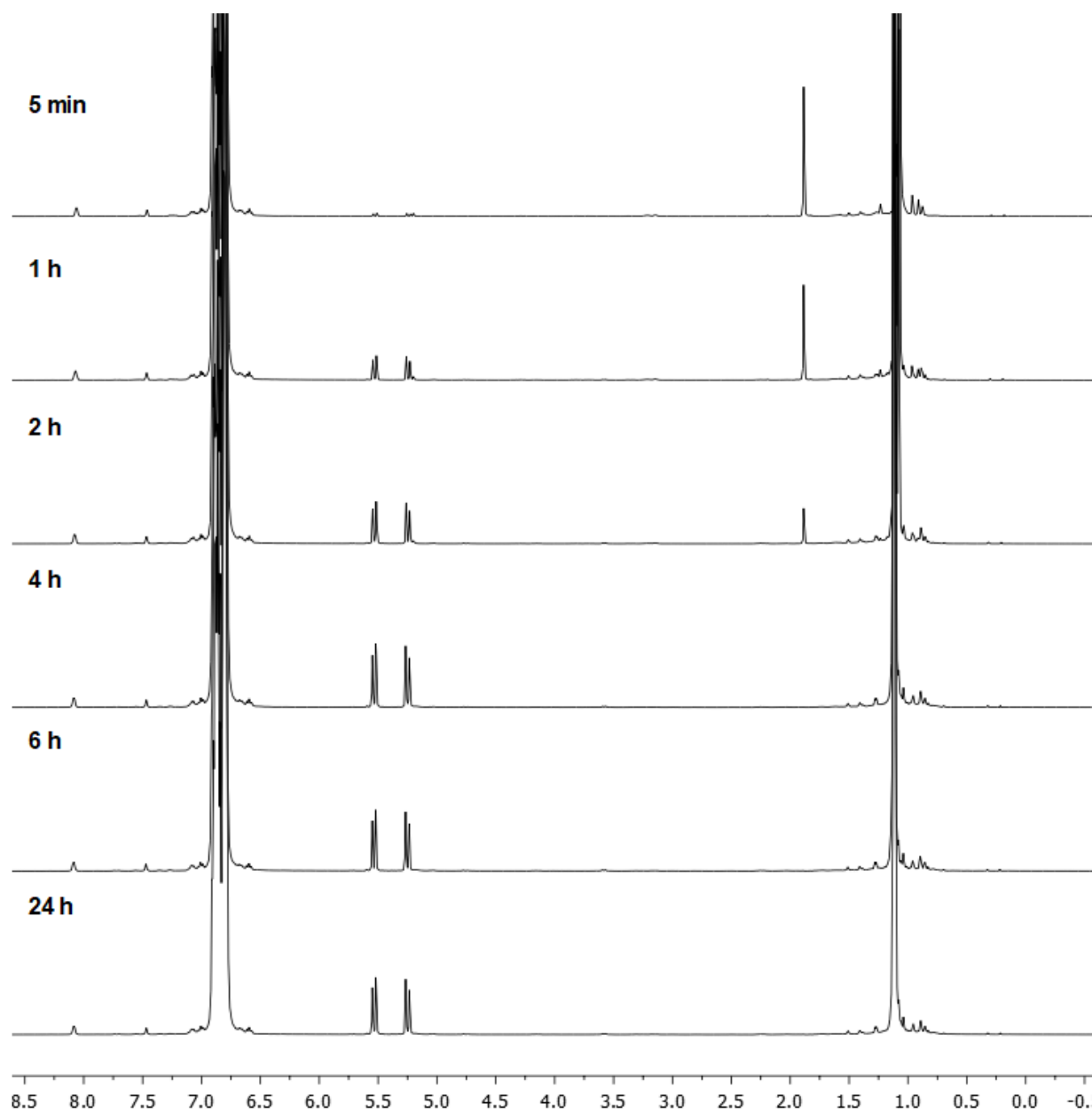


Figure S41. ¹H NMR spectra (DFB, 400 MHz) collected during the homocoupling of 3,3-dimethylbutyne promoted by **6** (1 mol%) and producing *Z*-*t*BuC≡CCHCH*t*Bu.

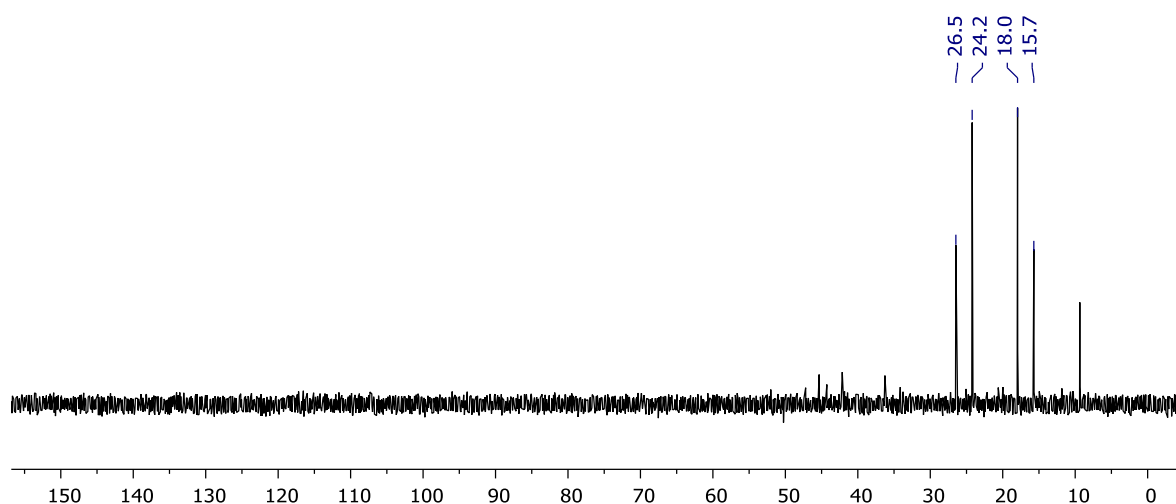


Figure S42. $^{31}\text{P}\{^1\text{H}\}$ NMR spectrum (DFB, 162 MHz) collected during the homocoupling of 3,3-dimethylbutyne promoted by **6** (1 mol%) and producing *Z*-*t*BuC \equiv CCHCH*t*Bu (6 h).

10 Preparation of $[\text{Ir}(\text{PNP-14})(\eta^3\text{-E-C}(\text{C}\equiv\text{CtBu})\text{CHtBu})(\eta^1\text{-E-CHCHtBu})][\text{BAR}^{\text{F}}_4]$ (**10**)

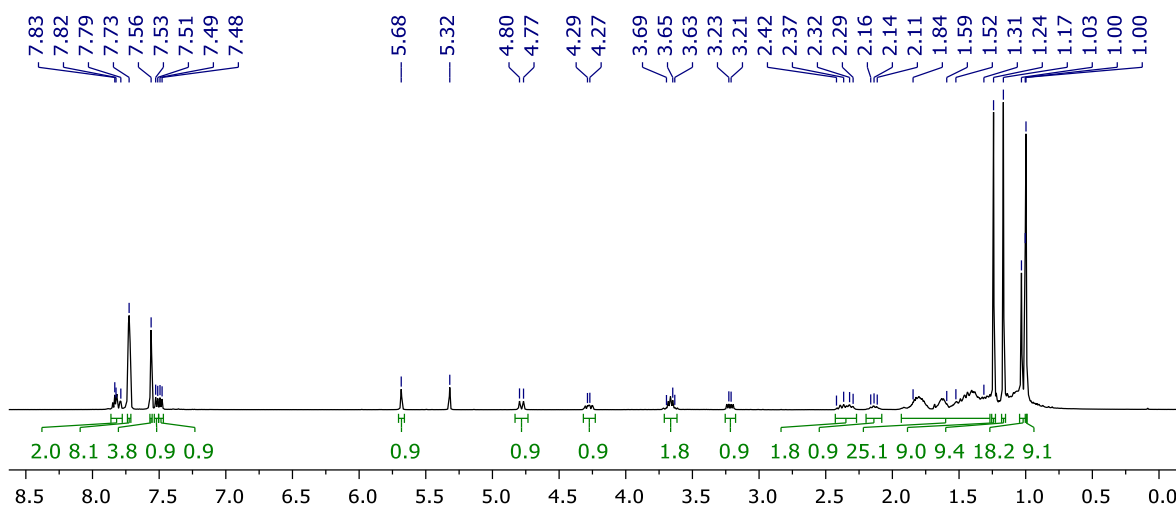


Figure S43. ^1H NMR spectrum of **10** (CD_2Cl_2 , 500 MHz).

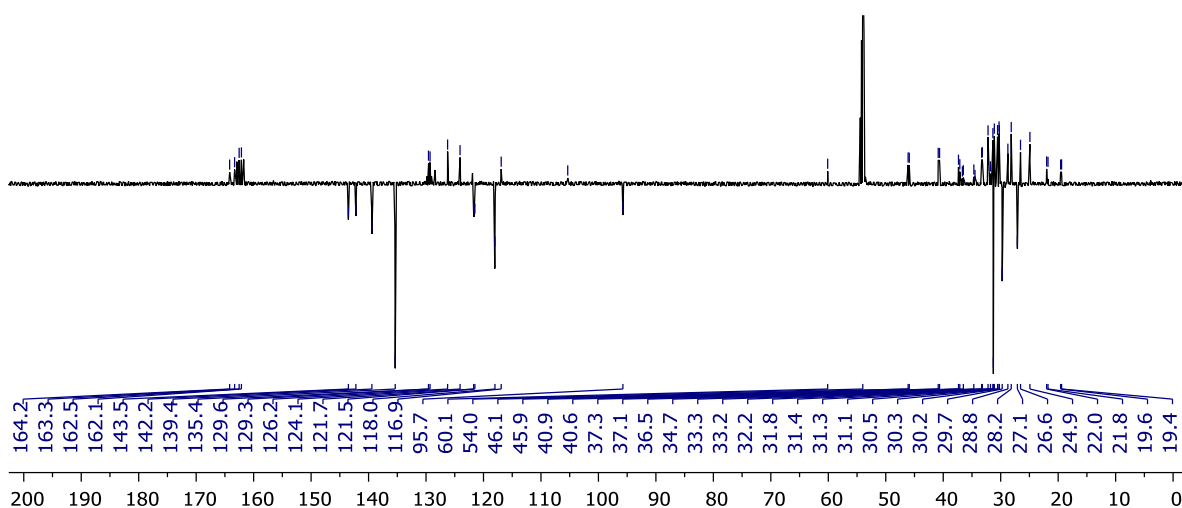


Figure S44. $^{13}\text{C}\{^1\text{H}\}$ APT NMR spectrum of **10** (CD_2Cl_2 , 126 MHz).

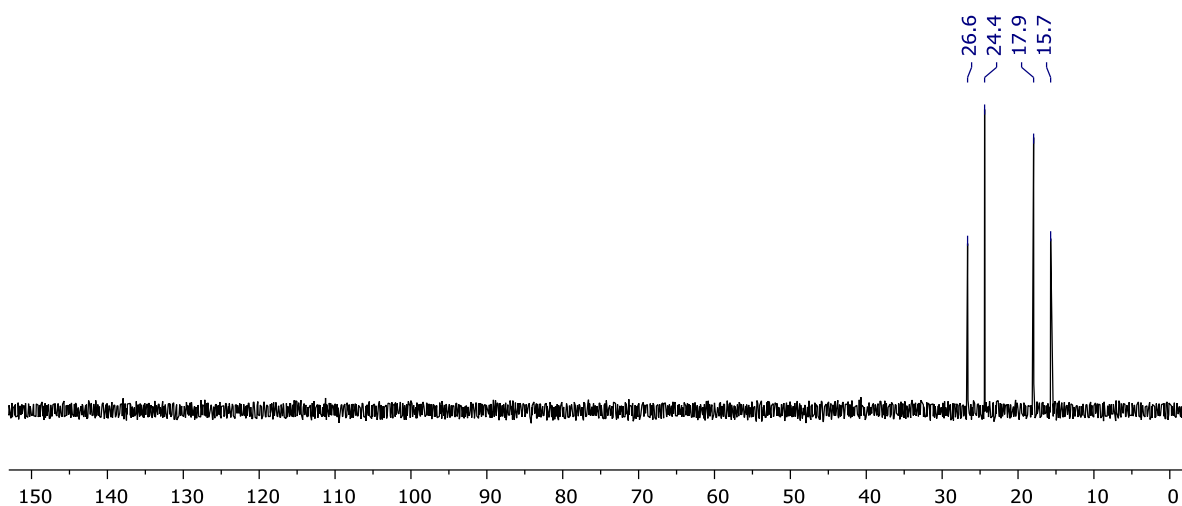


Figure S45. $^{31}\text{P}\{^1\text{H}\}$ NMR spectrum of **10** (CD_2Cl_2 , 162 MHz).

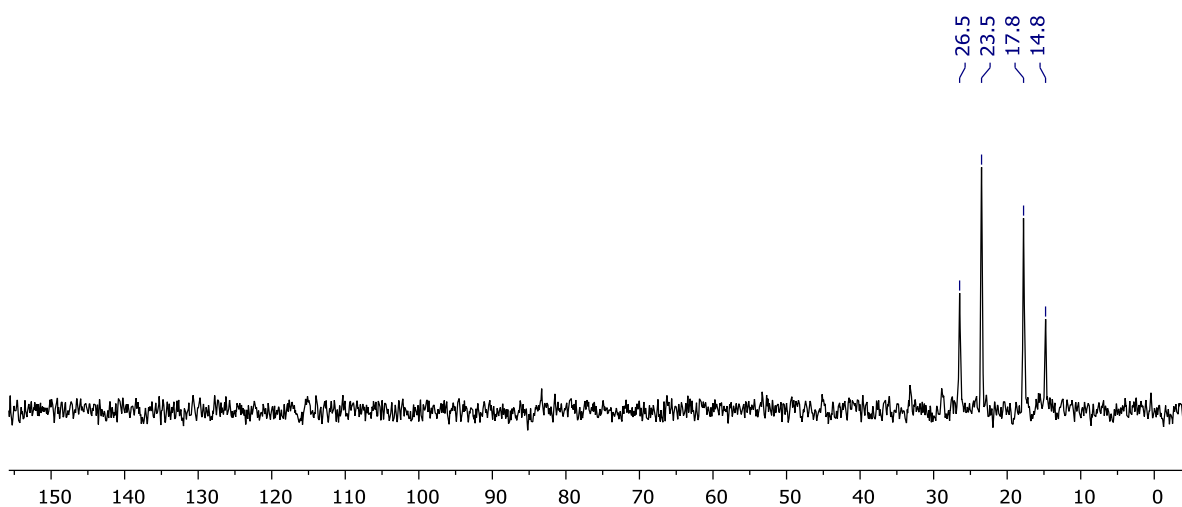


Figure S46. $^{31}\text{P}\{^1\text{H}\}$ NMR spectrum of **10** (DFB, 121 MHz).

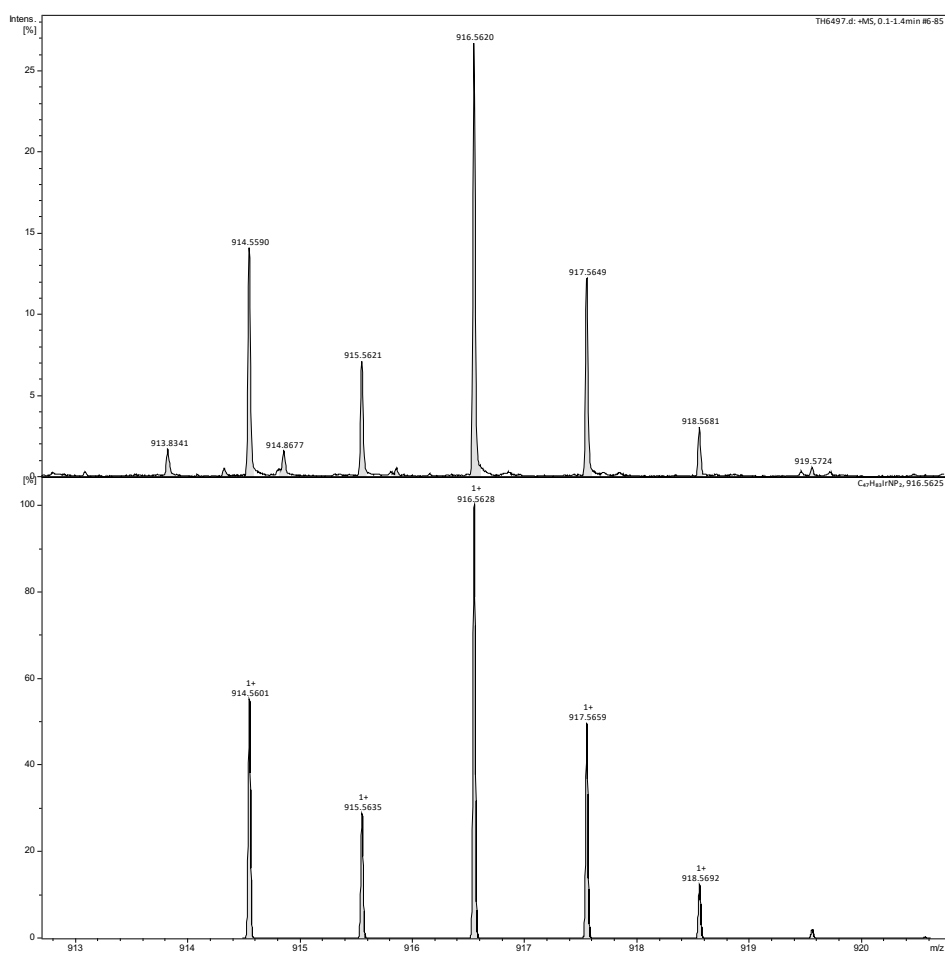


Figure S47. HR ESI-MS of **10**.

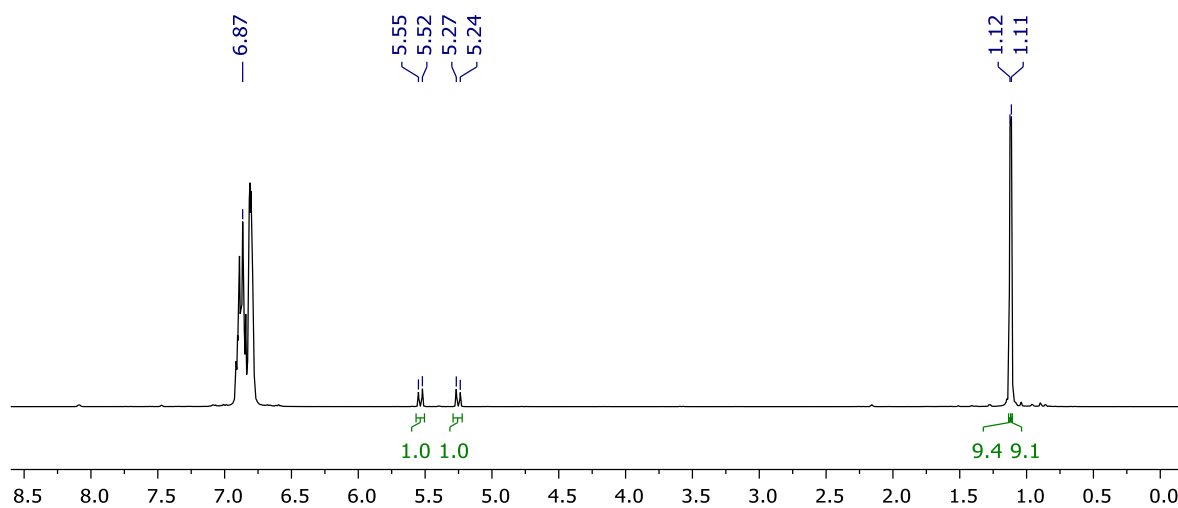


Figure S48. ^1H NMR spectrum of $Z\text{-}f\text{BuC}\equiv\text{CCHCH}f\text{Bu}$ isolated during the preparation of **10** (DFB, 400 MHz).

11 NMR scale reaction of **1** with Z - t BuC \equiv CCHCH t Bu

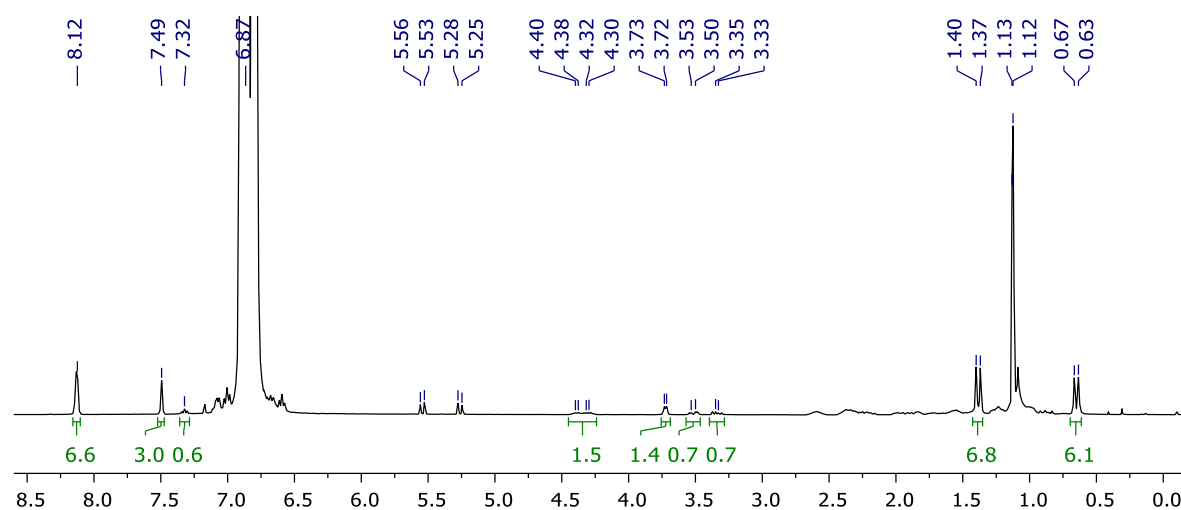


Figure S49. ^1H NMR spectrum of the reaction of **1** with Z - t BuC \equiv CCHCH t Bu (DFB, 400 MHz).

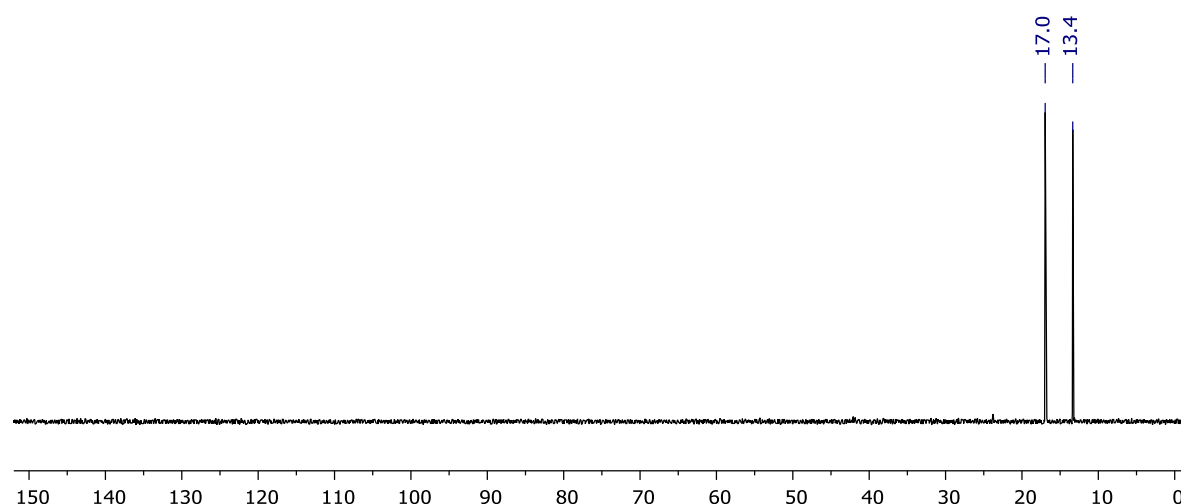


Figure S50. $^{31}\text{P}\{^1\text{H}\}$ NMR spectrum of the reaction of **1** with Z - t BuC \equiv CCHCH t Bu (DFB, 162 MHz).

12 Synthesis and characterisation of $[\text{Rh}(\text{PNP-14})(\eta^2\text{-norbornene})][\text{BAR}^{\text{F}}_4]$

A solution of $[\text{Rh}(\text{PNP-14})(\text{H}_2)][\text{BAR}^{\text{F}}_4]$ (18.6 μmol , generated *in situ* as described in *Dalton Trans.*, 2020, **49**, 2077 – 2086) in DFB (314 μL) was treated with a solution of norbornene in DFB (186 μL , 0.50 M, 93.0 μmol) and stirred at RT for 16 h. The volatiles were removed *in vacuo* and the resulting yellow oil washed with SiMe_4 (2×0.5 mL) and then dried under vacuum. Recrystallisation by slow diffusion of SiMe_4 into an Et_2O solution at 4 $^\circ\text{C}$ afforded the product as a yellow crystalline solid. Yield: 19.8 mg (12.9 μmol , 69%).

^1H NMR (500 MHz, DFB): δ 8.11 – 8.16 (m, 8H, Ar $^{\text{F}}$), 7.50 (br, 4H, Ar $^{\text{F}}$), 7.45 (t, $^3J_{\text{HH}} = 7.7$, 1H, py), 7.13 (obscured, 1H, py), 7.05 (obscured, 1H, py), 3.67 (app t, $J = 7$, 1H, Rh(CH=CH)), 3.03 – 3.30 (m, 5H, $4 \times \text{pyCH}_2 + 1 \times \text{Rh}(\text{CH=CH})$ [δ 3.15]), 2.84 (br d, $^3J_{\text{HH}} = 3.3$, 1H, CH{NBE}), 2.81 (br d, $^3J_{\text{HH}} = 3.4$, 1H, CH{NBE}), 0.90 – 2.39 (m, 32H, $\text{CH}_2 + 4 \times \text{CH}_2\text{CH}_2\{\text{NBE}\}$ [δ 1.51, 1.26; 1.39, 1.26]), 1.10 (d,

$^3J_{\text{PH}} = 13.9$, 9H, *t*Bu), 0.86 (br d, $^2J_{\text{HH}} = 9.1$, 1H, CHCH₂CH{NBE}), 0.81 (d, $^3J_{\text{PH}} = 13.5$, 9H, *t*Bu), 0.57 (br d, $^2J_{\text{HH}} = 9.0$, 1H, CHCH₂CH{NBE}).

$^{13}\text{C}\{^1\text{H}\}$ NMR (126 MHz, DFB): δ 163.1 (d, $^2J_{\text{PC}} = 8$, py), 162.6 (q, $^1J_{\text{CB}} = 50$, Ar^F), 161.2 (d, $^2J_{\text{PC}} = 7$, py), 138.1 (s, py), 135.1 (s, Ar^F), 129.7 (qq, $^2J_{\text{FC}} = 32$, $^3J_{\text{CB}} = 3$, Ar^F), 124.9 (q, $^1J_{\text{FC}} = 272$, Ar^F), 121.0 (d, $^3J_{\text{PC}} = 9$, py), 119.8 (d, $^3J_{\text{PC}} = 11$, py), 117.6 (sept, $^3J_{\text{FC}} = 4$, Ar^F), 66.7 (app t, $J = 10$, Rh(CH=CH)), 62.9 (dd, $J = 10, 8$, Rh(CH=CH)), 47.1 (s, CH{NBE}), 44.4 (d, $J = 2$, CH{NBE}), 41.0 (d, $J = 2$, CHCH₂CH{NBE}), 39.0 (dd, $^1J_{\text{PC}} = 19$, pyCH₂), 38.3 (d, $^1J_{\text{PC}} = 18$, pyCH₂), 34.4 (d, $^1J_{\text{PC}} = 18$, *t*Bu{C}), 33.6 (dd, $^1J_{\text{PC}} = 15$, $^3J_{\text{PC}} = 6$, *t*Bu{C}), 31.6 (d, $^2J_{\text{PC}} = 11$, CH₂), 30.2 (d, $^2J_{\text{PC}} = 10$, CH₂), 30.1 (s, CH₂), 29.8 (s, CH₂), 29.5 (s, CH₂), 29.3 (s, 2×CH₂), 28.6 (s, CH₂), 27.9 (s, CH₂), 27.7 (s, CH₂), 27.5 (s, CH₂), 27.4 (d, $^2J_{\text{PC}} = 4$, *t*Bu{CH₃}), 27.2 (d, $^2J_{\text{PC}} = 5$, *t*Bu{CH₃}), 26.9 (s, CH₂), 26.6 (s, CH₂), 25.1 (br d, $^1J_{\text{PC}} = 16$, PCH₂), 23.9 (d, $^3J_{\text{PC}} = 2$, CH₂), 20.7 (br d, $^1J_{\text{PC}} = 23$, PCH₂).

$^{31}\text{P}\{^1\text{H}\}$ NMR (162 MHz, DFB): δ 71.2 (dd, $^2J_{\text{PP}} = 244$, $^1J_{\text{RhP}} = 131$, 1P), 55.9 (dd, $^2J_{\text{PP}} = 244$, $^1J_{\text{RhP}} = 125$, 1P).

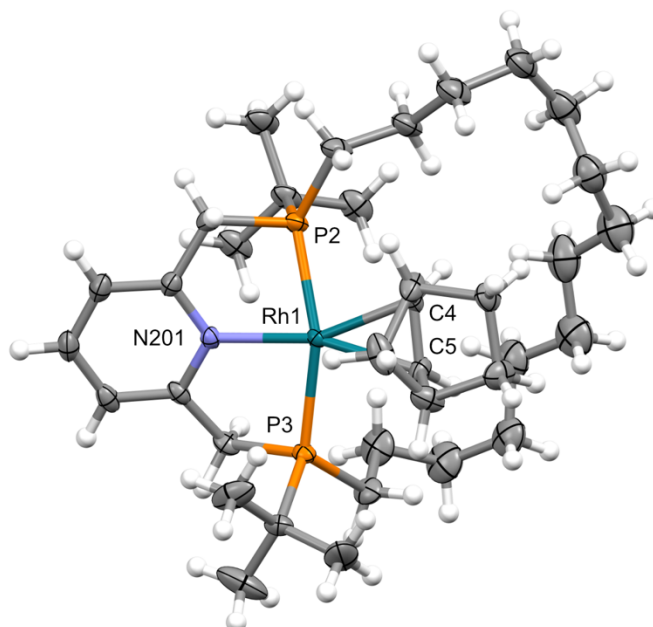


Figure S51. Solid-state structure of [Rh(PNP-14)(η^2 -norbornene)][BARF₄]; thermal ellipsoids at 30% probability; anion omitted. Selected bond lengths (Å) and angles (°): Rh1-P2, 2.2916(8); Rh1-P3, 2.3118(7); P2-Rh1-P3, 153.11(3); Rh1-N201, 2.088(2); Rh1-Cnt(C4,C5), 2.085(3); N201-Rh1-Cnt(C4,C5), 169.19(11); Cnt = centroid.

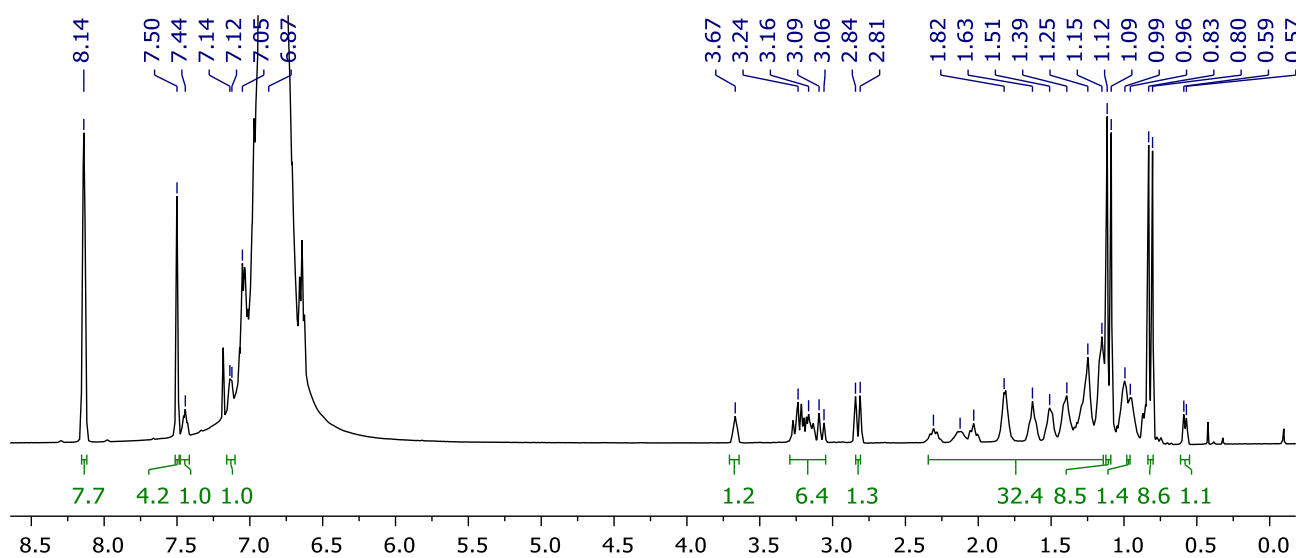


Figure S52. ^1H NMR spectrum of $[\text{Rh}(\text{PNP-14})(\eta^2\text{-norbornene})][\text{BARF}_4]$ (DFB, 500 MHz).

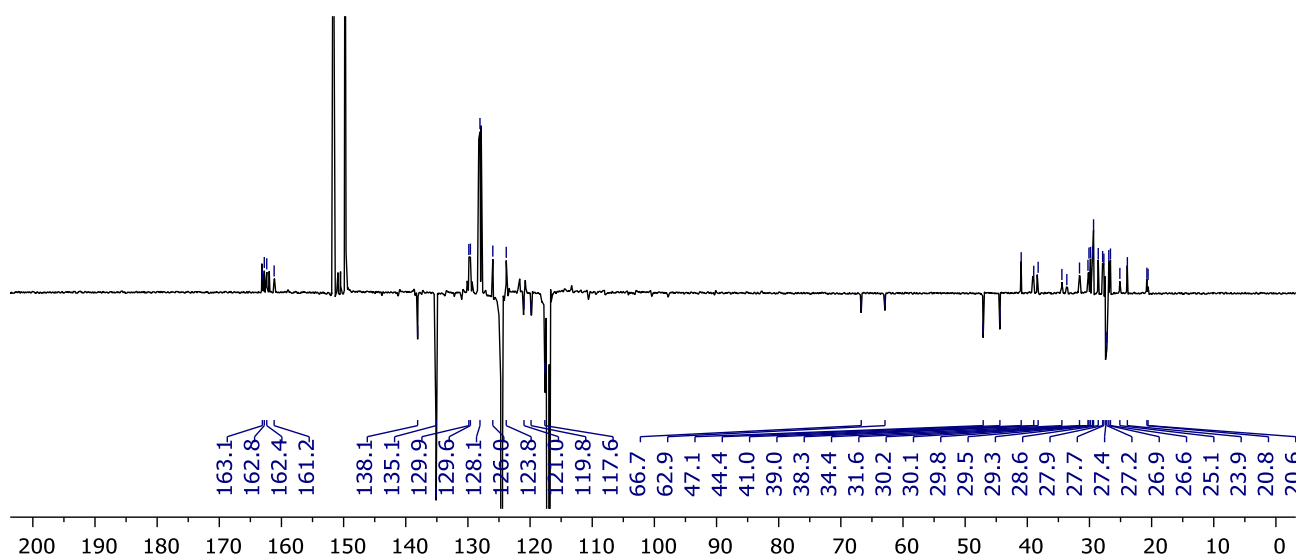


Figure S53. $^{13}\text{C}\{^1\text{H}\}$ APT NMR spectrum of $[\text{Rh}(\text{PNP-14})(\eta^2\text{-norbornene})][\text{BARF}_4]$ (DFB, 126 MHz).

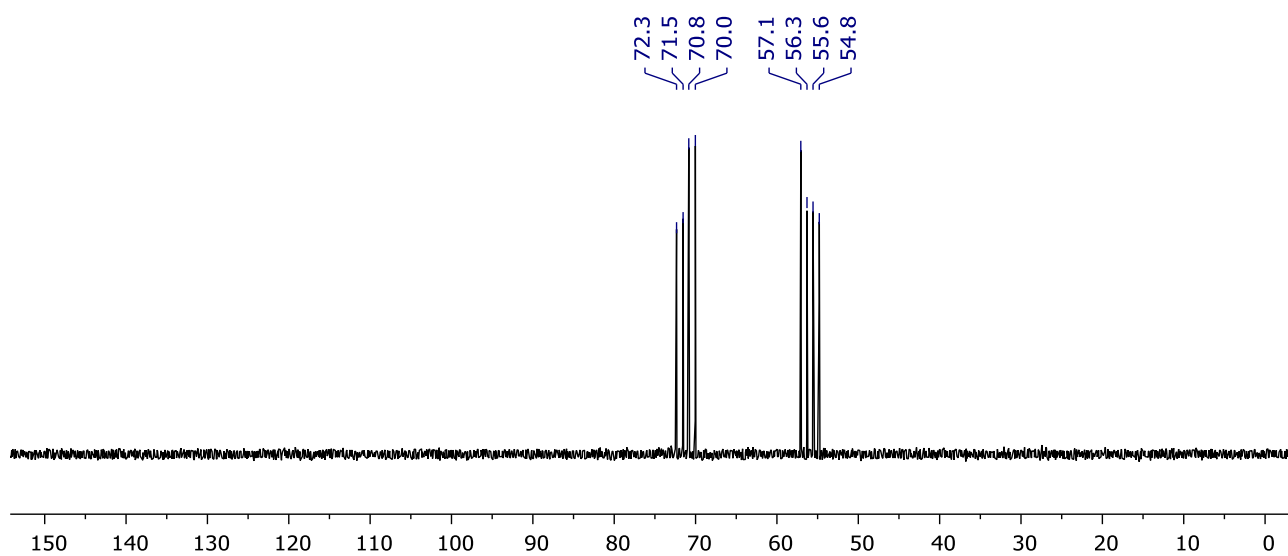


Figure S54. $^{31}\text{P}\{^1\text{H}\}$ NMR spectrum of $[\text{Rh}(\text{PNP-14})(\eta^2\text{-norbornene})][\text{BARF}_4]$ (DFB, 162 MHz).